NASA TN D-1824

TECHNICAL NOTE

D-1824

USE OF AERODYNAMIC PARAMETERS FROM NONLINEAR THEORY IN MODIFIED-STRIP-ANALYSIS FLUTTER CALCULATIONS FOR FINITE-SPAN WINGS AT SUPERSONIC SPEEDS

By E. Carson Yates, Jr., and Robert M. Bennett

Langley Research Center
Langley Station, Hampton, Va.

NATIONAL AERONAUTICS AND SPACE ADMINISTRATION

WASHINGTON July 1963

NATIONAL AERONAUTICS AND SPACE ADMINISTRATION

TECHNICAL NOTE D-1824

USE OF AERODYNAMIC PARAMETERS FROM NONLINEAR THEORY IN MODIFIED-STRIP-ANALYSIS FLUTTER CALCULATIONS FOR FINITE-SPAN WINGS AT SUPERSONIC SPEEDS

By E. Carson Yates, Jr., and Robert M. Bennett

SUMMARY

The flutter characteristics for two untapered wings, one having 15° sweep and aspect ratio 5.34, the other having 30° sweep and aspect ratio 4.16, have been investigated analytically for Mach numbers up to 3.0. The calculations were based on the modified-strip-analysis method of NACA Research Memorandum L57L10 with the required aerodynamic parameters computed from linear theory, from shock-expansion theory, and from Busemann second-order theory. The results were compared with flutter experiments over the Mach number range. Supersonic flutter speeds were satisfactorily predicted by the modified strip analysis employing aerodynamic parameters computed from the nonlinear theories but were high when supersonic linear theory was used. Flutter speeds calculated for subsonic Mach numbers by use of linear-theory aerodynamic parameters were in good agreement with experimental values.

INTRODUCTION

Difficulties in formulating and using rigorous aerodynamic theories for unsteady, three-dimensional, compressible flow have led to widespread use of approximate methods for evaluating the oscillatory aerodynamic loads required in flutter analyses. One of these approximate methods is the modified strip analysis[1] presented in reference 1. This method, which is limited to relatively

[1]In this method, spanwise distributions of steady-flow section lift-curve slope and local aerodynamic center for the undeformed wing are used in conjunction with the "effective" angle-of-attack distribution resulting from the assumed vibration modes in order to obtain values of section lift and pitching moment. The steady-state aerodynamic parameters may be obtained from any suitable theory or experiment, the criterion being that the best method to use is the one that yields the most accurate steady-state load distributions. Circulation functions modified on the basis of loadings for two-dimensional airfoils oscillating in compressible flow are employed to account for the effects of oscillatory motion on the magnitudes and phase angles of the lift and moment vectors. Some characteristics of resulting oscillatory section lift and pitching moment are examined briefly in the appendix of the present report.

low reduced frequencies, was applied in reference 1 to a number of swept and unswept wings for Mach numbers from zero to as high as 1.75. The results showed generally good agreement with experimental flutter data, thus indicating the usefulness of this comparatively simple procedure especially for trend-study and preliminary-design information. It is quite obvious, however, that such an approximate method is intended to supplement rather than to supplant the more rigorous theoretical techniques.

The aerodynamic coefficients employed in all of the calculations of reference 1 were obtained from linearized aerodynamic theory. However, use of linearized aerodynamic theory in the modified strip analysis may be expected to yield less accurate flutter characteristics as Mach number increases. First, it is well known that for wings of finite thickness, linearized aerodynamic theory predicts pressure distributions and hence aerodynamic-center positions with decreased accuracy at the higher supersonic Mach numbers. (See refs. 2 to 4, for example.) Furthermore, the results of reference 5 indicate that as Mach number increases, the calculated flutter speed and frequency become more sensitive to small changes in local aerodynamic-center position. It is thus apparent that the calculation of accurate flutter characteristics at the higher supersonic Mach numbers will require the use of aerodynamic parameters obtained from the more accurate nonlinear aerodynamic theories or from experiments (ref. 6).

The primary objectives of the present report are to illustrate the use of nonlinear aerodynamics in conjunction with the flutter-analysis method of reference 1 and to examine the accuracy of the resulting flutter characteristics. For these purposes supersonic flutter characteristics have been calculated for two untapered swept wings by the method of reference 1 with the required aerodynamic coefficients obtained from linear theory, from Busemann second-order theory, and from shock-expansion theory. The calculations cover Mach numbers up to 3.0 and are compared with the experimental flutter data given in reference 7 for these wings. The results of extensive supersonic flutter calculations for these wings by piston theory and by quasi-steady second-order theory are presented in reference 8.

For completeness some calculations have been made for these two wings at subsonic Mach numbers by the modified strip method of reference 1 using linear-theory aerodynamic coefficients. The subsonic flutter characteristics of these wings have also been investigated by use of the subsonic kernel function method (results unpublished).

SYMBOLS

$a_{c,n}$ nondimensional distance from midchord to local aerodynamic center (for steady flow at zero angle of attack) measured perpendicular to elastic axis, positive rearward; fraction of semichord perpendicular to elastic axis (called ac_n in ref. 1)

b_s semichord measured streamwise

$c_{l_{\alpha,n}}$ local lift-curve slope for a section perpendicular to elastic axis in steady flow at zero angle of attack

$c_{m_{\alpha,n}}$ derivative with respect to angle of attack of local pitching-moment coefficient measured about leading edge of a section perpendicular to the elastic axis in steady flow at zero angle of attack

K_L ratio of $(c_{l_{\alpha,n}})_{2D}$ calculated by nonlinear theory to $(c_{l_{\alpha,n}})_{2D}$ calculated by linear theory

K_M ratio of $(c_{m_{\alpha,n}})_{2D}$ calculated by nonlinear theory to $(c_{m_{\alpha,n}})_{2D}$ calculated by linear theory

k reduced frequency, $\frac{b_s\omega}{V}$

M Mach number

M_{le} Mach number component normal to leading edge

$\overline{m}$ total mass of wing panel

V flutter speed

v volume of air within a cylinder having streamwise chord as base diameter and panel span as height

η distance measured from wing root along elastic axis, fraction of elastic axis length

$\bar{\mu}$ mass ratio for wing panel, $\frac{\overline{m}}{\rho v}$

ρ air density

ω circular frequency of vibration at flutter

ω_k circular frequency of kth natural (coupled) vibration mode

$\omega_{h,i}$ circular frequency of ith uncoupled bending vibration mode

ω_α circular frequency of first uncoupled torsional vibration mode

$\left|\frac{dc_l}{d\alpha}\right|$ amplitude of the oscillatory section lift-curve slope

$\left|\frac{dc_m}{d\alpha}\right|$ amplitude of the oscillatory section pitching-moment-curve slope, pitching moment measured about pitch axis

θ_α phase angle between oscillatory section lift and pitch angle measured from free-stream direction

$\theta_{\alpha m}$ phase angle between oscillatory section pitching moment and pitch angle measured from free-stream direction

Subscripts:

2D two dimensional

3D three dimensional

DESCRIPTION OF WINGS

General Description

The flutter calculations of this report were made for two of the untapered, swept wings for which experimental flutter data were given in reference 7. One wing was swept back 15° and had an aspect ratio of 5.34; the other was swept back 30° and had an aspect ratio of 4.16. (See fig. 1.) These wings were cut from 0.041-inch-thick aluminum or magnesium sheet and had chords of 2 inches measured perpendicular to the leading edge. As shown in figure 1, the leading and trailing edges of both wings were beveled 1/4 inch to form a 2.05-percent-thick symmetrical hexagonal airfoil section perpendicular to the leading edge. For these homogeneous untapered wings, both the elastic axis and the local centers of gravity were taken to be at midchord.

In the investigations of reference 7, two magnesium models and two aluminum models of each planform were flutter tested. Since flutter calculations are presented herein for all of these models, they have been arbitrarily designated as models A, B, C, and D for convenient reference. (See table I.) Note specifically that models A, B, and C are the same as models A, B, and C of reference 8.

Mode Shapes and Frequencies

Uncoupled beam-type vibration modes were employed in all flutter calculations. Since the wings investigated herein were homogeneous and untapered, the uncoupled mode shapes and frequencies for both planforms were considered to be the same as those for a uniform cantilever beam. The uncoupled bending-mode and torsion-mode frequencies for 15° wing models A and C and for 30° wing models A and C were calculated from the simple formulas for a uniform cantilever beam. To allow for slight differences in stiffness between ostensibly identical models A and B, the uncoupled-mode frequencies for model B were obtained from those for model A by multiplying by the ratio of the measured first-natural-mode frequency of model B to the corresponding frequency of model A. That is, for model B

$$(\omega_{h,i})_B = \frac{(\omega_1)_B}{(\omega_1)_A}(\omega_{h,i})_A$$

and

$$(\omega_\alpha)_B = \frac{(\omega_1)_B}{(\omega_1)_A}(\omega_\alpha)_A$$

Similarly, for model D

$$(\omega_{h,i})_D = \frac{(\omega_1)_D}{(\omega_1)_C}(\omega_{h,i})_C$$

and

$$(\omega_\alpha)_D = \frac{(\omega_1)_D}{(\omega_1)_C}(\omega_\alpha)_C$$

The uncoupled-mode frequencies for all models are presented in table I. For each model, the frequency of the second bending mode is close to that of the first torsion mode, and both are near the measured second- and third-mode natural (coupled) frequencies given in reference 7. (See also table I herein.)

The first three measured natural (coupled) mode shapes for these wings presented in reference 9 and the corresponding node lines (fig. 1) indicate that the second and third natural modes involve a high degree of bending-torsion coupling, particularly for the 30° wing. In addition, the mode shapes show that some camber occurs in some of the modes. Since the natural modes are not closely approximated by uncoupled modes, a question arises with regard to the suitability of uncoupled modes for the flutter analyses. Reference 1 indicated that the modified strip analysis could be formulated to employ coupled vibration modes; furthermore, a camber mode could also be employed. These provisions, however, are not included in the method as presently programed; therefore, a direct comparison of coupled-mode and uncoupled-mode strip-theory calculations was not feasible. However, little difference occurred between coupled-mode and uncoupled-mode subsonic kernel-function calculations for these two wings (results unpublished).

In comparison, the flutter analyses for the swept wings of reference 10 also indicated little difference between flutter speeds obtained from coupled natural-mode and uncoupled beam-mode calculations by the subsonic kernel function method, even though the natural modes for those wings contained considerably more camber than the modes for the present wings. The results of both types of kernel-function calculations as well as of modified-strip-theory calculations (with uncoupled modes) were in good agreement with experiment (ref. 10).

Finally, it may be noted that even when uncoupled vibration modes are used in the analyses of swept wings, some camber is included in the deflections along streamwise sections. For uncoupled modes, wing sections normal to the elastic

axis are assumed to oscillate without distortion. Therefore, if these sections do not lie in the free-stream direction, some camber deformation of streamwise sections appears.

FLUTTER CALCULATIONS

The modified-strip-analysis method employed herein is described in reference 1. The procedure of this report differs from that of reference 1 only with regard to the method of calculating the aerodynamic parameters $c_{l_{\alpha,n}}$ and $a_{c,n}$. For the wings of this report, values of $c_{l_{\alpha,n}}$ and $a_{c,n}$ were computed by three methods for supersonic Mach numbers and two methods for subsonic Mach numbers as indicated in table II.

In most of the flutter calculations by the modified-strip-analysis method, three uncoupled vibration modes were used - first and second bending and first torsion. However, the third bending mode was included in one calculation for 15° wing model B for comparison with the three-mode results.

Supersonic Speed Range

Linearized theory.- In the supersonic speed range, aerodynamic parameters were calculated by the linearized lifting-surface method of reference 11, since the leading edges of both wing planforms were supersonic at all Mach numbers calculated. For the 15° wing, the required distributions of $c_{l_{\alpha,n}}$ and $a_{c,n}$ for wing sections normal to the elastic axis were initially obtained from corresponding values for streamwise sections by application of simple sweep theory as described in reference 1. Subsequently, the values of $c_{l_{\alpha,n}}$ and $a_{c,n}$ were reevaluated by direct integration of lifting pressure along sections normal to the elastic axis. Results of these two evaluations are compared in figure 2. The close agreement at all Mach numbers was anticipated because the wing was untapered and swept only 15°. The small differences shown would be expected to cause negligible change in the calculated flutter characteristics. The two preceding statements would not be valid, however, for a highly tapered wing with significantly greater sweepback, as was demonstrated in reference 10. The values of $c_{l_{\alpha,n}}$ and $a_{c,n}$ obtained by use of simple sweep theory (fig. 2) were used in the present flutter calculations for the 15° wing because they were available earlier than values obtained by direct integration. For the 30° wing, however, all calculations of $c_{l_{\alpha,n}}$ and $a_{c,n}$ by supersonic linearized aerodynamic theory (fig. 3) were made by direct integration of lifting pressure along sections perpendicular to the elastic axis.

Nonlinear theories.- No general theory is known to exist for evaluating the nonlinear aerodynamic effects of finite wing thickness and airfoil shape on the supersonic steady-flow aerodynamic loads on finite-span wings. For use in the present flutter analyses, therefore, such nonlinear effects on the distributions

of $c_{l_{\alpha,n}}$ and $a_{c,n}$ are approximated by employing two-dimensional nonlinear theory to modify the spanwise distributions of aerodynamic parameters calculated from three-dimensional linearized theory. Approximations of this type were also employed in references 12 and 13. Specifically herein, the values of section lift-curve slope $c_{l_{\alpha,n}}$ obtained from three-dimensional linear theory were multiplied by the ratio of $c_{l_{\alpha,n}}$ obtained from two-dimensional nonlinear theory to $c_{l_{\alpha,n}}$ obtained from two-dimensional linear theory; that is,

$$\left(c_{l_{\alpha,n}}\right)_{3D,\text{nonlinear}} = \left[\frac{\left(c_{l_{\alpha,n}}\right)_{2D,\text{nonlinear}}}{\left(c_{l_{\alpha,n}}\right)_{2D,\text{linear}}}\right]\left(c_{l_{\alpha,n}}\right)_{3D,\text{linear}}$$

$$= K_L\left(c_{l_{\alpha,n}}\right)_{3D,\text{linear}} \tag{1}$$

Similarly for the section pitching-moment slope $c_{m_{\alpha,n}}$,

$$\left(c_{m_{\alpha,n}}\right)_{3D,\text{nonlinear}} = \left[\frac{\left(c_{m_{\alpha,n}}\right)_{2D,\text{nonlinear}}}{\left(c_{m_{\alpha,n}}\right)_{2D,\text{linear}}}\right]\left(c_{m_{\alpha,n}}\right)_{3D,\text{linear}}$$

$$= K_M\left(c_{m_{\alpha,n}}\right)_{3D,\text{linear}} \tag{2}$$

Using values of $c_{l_{\alpha,n}}$ and $c_{m_{\alpha,n}}$ obtained from equations (1) and (2), the local aerodynamic-center positions $\left(a_{c,n}\right)_{3D,\text{nonlinear}}$ were calculated from

$$\left(a_{c,n}\right)_{3D,\text{nonlinear}} = 2\,\frac{\left(c_{m_{\alpha,n}}\right)_{3D,\text{nonlinear}}}{\left(c_{l_{\alpha,n}}\right)_{3D,\text{nonlinear}}} - 1 \tag{3}$$

In all of these calculations, the two-dimensional aerodynamic parameters were computed for wing sections normal to the elastic axis and for the Mach number component normal to the leading edge. This Mach number component was chosen because the nature of the pressure distribution over the wing is dominantly affected by whether the leading edge is subsonic or supersonic. (See also ref. 1.)

The two nonlinear two-dimensional aerodynamic theories employed herein are the complete shock-expansion theory as presented in reference 14, and the Busemann second-order theory as used in references 12 and 13. Steady-state aerodynamic load distributions calculated by shock-expansion theory for wings with sharp leading edges have been shown to agree well with measured values at the higher supersonic Mach numbers. (See ref. 15, for example.) Although the Busemann

second-order theory lacks the theoretical exactness of the complete shock-expansion theory, the simplicity of application of the second-order theory would make it attractive for use in flutter analyses if the results can be shown to be sufficiently accurate.

The shock-expansion theory is directly applicable only to sharp-edge airfoils at Mach numbers for which the leading-edge shock wave is attached. These limitations did not affect the present applications to the 15° and 30° wings because both were sharp edged and because the leading-edge bevel on both yielded wedge angles small enough to permit shock attachment at relatively low supersonic Mach numbers. For wings with round leading edges, however, the shock-expansion theory as presented in reference 14 can be applied approximately by employing the artifice of the sonic wedge tangent on the airfoil nose (ref. 16). Compared with values obtained from two-dimensional linear theory, the values of $c_{m_{\alpha,n}}$ obtained from shock-expansion theory are significantly altered in the present application $(K_M < 1.00)$; however, the $c_{l_{\alpha,n}}$ values were only slightly affected, differing in the present cases by less than 2 percent $(1.00 < K_L < 1.02)$. The airfoil sections normal to the leading edge were identical for the 15° and 30° wings so that the same shock-expansion-theory calculations were applicable to both. The values of $(a_{c,n})_{2D,\text{shock expansion}}$ were calculated from the following equation:

$$(a_{c,n})_{2D,\text{nonlinear}} = 2\frac{\left(c_{m_{\alpha,n}}\right)_{2D,\text{nonlinear}}}{\left(c_{l_{\alpha,n}}\right)_{2D,\text{nonlinear}}} - 1 \qquad (4)$$

and are shown in figure 4. It can be seen that even for the present thin wings (2.05 percent thick measured perpendicular to the leading edge), the shock-expansion theory yields aerodynamic-center positions significantly forward of those indicated by linear theory $\left((a_{c,n})_{2D,\text{linear}} = 0\right)$. Distributions of $(a_{c,n})_{3D,\text{shock expansion}}$ obtained from these values are compared with those from linear-theory calculations in figures 2 and 3. Values of $\left(c_{l_{\alpha,n}}\right)_{3D,\text{shock expansion}}$ are not shown in figures 2 and 3 because of their closeness to the linear-theory curves.

Unlike the shock-expansion theory, the Busemann second-order theory causes no change at all from the linear-theory value of the lift-curve slope $(K_L \equiv 1.00)$ and yields a change in $c_{m_{\alpha,n}}$ $(K_M < 1.00)$ that is a function only of Mach number and airfoil cross-sectional area. Thus the problem of airfoil nose shape is not directly encountered even though the theory is strictly applicable only to sharp-nose sections. Values of $(a_{c,n})_{2D,\text{second order}}$ for the airfoil (normal to the leading edge) of the present wings were calculated from equation (4) and are shown in figure 4. The aerodynamic centers calculated by the Busemann second-order theory are appreciably forward of the positions indicated by linear theory, but are not as far forward as the positions obtained from the shock-expansion theory. The values of $(a_{c,n})_{2D}$ obtained from Busemann second-order theory for

an NACA 65A002 airfoil are also shown in figure 4 to illustrate the effect of differing cross-sectional areas for two airfoils with approximately the same maximum thickness.

Subsonic Speed Range

Flutter calculations for both the 15° and 30° wings at subsonic Mach numbers followed the procedure outlined in reference 1. In particular, the required distributions of $c_{l_{\alpha,n}}$ were computed by the lifting-line method of reference 17 and are shown in figures 2 and 3. Note specifically that this method implicitly places the local aerodynamic centers along the streamwise quarter-chord line, so that, for the present untapered wings, $a_{c,n} = -1/2$. The importance of this restriction on local aerodynamic center and hence on section pitching moment, was examined for the 15° wing. For this purpose, some flutter calculations for this wing employed distributions of $c_{l_{\alpha,n}}$ and $a_{c,n}$ calculated by subsonic lifting-surface theory, essentially that of reference 18. These values of $c_{l_{\alpha,n}}$ and $a_{c,n}$ are compared with the values obtained from the lifting-line theory in figure 2. For all three subsonic Mach numbers and for all values of η, $c_{l_{\alpha,n}}$ obtained from lifting-surface theory is shown to be slightly higher than the corresponding values obtained from lifting-line theory. Moreover, the aerodynamic-center positions indicated by lifting-surface theory are farther forward than those associated with lifting-line theory, particularly near the wing tip. The results of reference 5 indicate that both of these differences would be expected to have depressing effects on the calculated flutter speeds when compared with flutter speeds obtained by use of lifting-line theory.

RESULTS AND DISCUSSION

A summary of pertinent conditions for all the calculations and an index to the results are provided in table II. The flutter speeds and frequencies calculated by the modified-strip analysis employing aerodynamic parameters obtained from both linear and nonlinear aerodynamic theories are compared with experimental flutter data from reference 7 in figures 5 and 6 for the 15° wing and in figures 7 and 8 for the 30° wing. In the calculations of all the flutter speed and flutter frequency curves of figures 5 to 8, the wing properties and flow density employed were those associated with the experimental flutter points shown. Since each experimental point (from ref. 7) represents a different model and a different density, the calculations for each model and density were limited to a range of Mach number which bracketed the experimental value. The range of Mach number covered for each model is indicated in table II. Because of the discontinuous change of mass ratio and modal frequencies at the extremities of these Mach number ranges, the calculated flutter characteristics also show discontinuities at these locations.

Supersonic Speed Range

Results of the flutter calculations which employed aerodynamic parameters computed from linearized supersonic-flow theory are included in figures 5 to 8. Both the flutter speeds and frequencies calculated from these values of $c_{l_{\alpha,n}}$ and $a_{c,n}$ are appreciably higher than experiment for the 15° wing all through the supersonic range and for the 30° wing at the higher supersonic Mach numbers. This observation is in agreement with the results of references 5 and 6 in which supersonic linear theory characteristically predicted aerodynamic-center positions that were too far rearward and these in turn characteristically yielded flutter speeds that were too high. However, for the 30° wing the agreement of the calculations with experiment at low supersonic Mach numbers is good. The larger sweep angle of this wing decreases the Mach number component normal to the leading edge and increases the portion of the wing area that is behind the Mach line from the root leading edge. Hence, at a given low supersonic Mach number the local aerodynamic centers for this wing are farther forward than those for the 15° wing (for example, compare figs. 2(e) and 3(d)). The calculated flutter characteristics for the 30° wing are therefore less sensitive to small variations in $a_{c,n}$. (See ref. 5.)

For both wings the differences between experimental flutter speeds and those calculated from linear-theory aerodynamics progressively increase with increasing supersonic Mach number. For these wings the elastic axes and local centers of gravity were at midchord so that the aerodynamic centers could never move rearward of them. Hence, no change of sign in the calculated section pitching moment occurred as it did for the 45° swept wing of reference 10, and the accompanying sharp upward break of calculated flutter speed with increasing Mach number (ref. 10) was not encountered here. Nevertheless, for the present moderately swept wings the local aerodynamic centers did move rearward to the vicinity of the elastic axis and the local centers of gravity even at relatively low supersonic Mach numbers. Under these conditions accurate flutter prediction by the modified strip method even at moderately low supersonic speeds requires the aerodynamic centers to be located more accurately than is possible by use of linearized aerodynamic theory.

The flutter calculations incorporating values of $c_{l_{\alpha,n}}$ and $a_{c,n}$ computed from shock-expansion theory are also shown in figures 5 to 8. The agreement between the calculated and experimental flutter speeds is good over the Mach number range. Thus, the more accurate determination of $c_{l_{\alpha,n}}$ and especially $a_{c,n}$ by shock-expansion theory yields considerable improvement in the calculated flutter speeds.

Figures 5 to 8 also include flutter characteristics calculated for the 15° and 30° wings with $a_{c,n}$ values computed from Busemann second-order theory. Over the Mach number range, the calculated flutter speeds are in fair agreement with experimental values for the 15° wing. Corresponding results for the 30° wing show good agreement with experiment. These calculated flutter speeds, however, are higher than those calculated by using shock-expansion theory as would be expected (ref. 5) since the aerodynamic centers obtained from Busemann

second-order theory (figs. 2 and 4) are rearward of the values given by shock-expansion theory. The Busemann second-order-theory correction to the aerodynamic-center position is a function only of the airfoil cross-sectional area and of two Mach number dependent coefficients which are given, for example, in equations (3-11), section E, of reference 19. As indicated previously, this theory may be applied more expediently than the shock-expansion theory, and hence may be preferable in cases for which some conservativeness may be sacrificed for greater simplicity in the calculations.

As stated previously, most of the present flutter calculations employed three vibration modes (first torsion and first and second bending). However, a single calculation for the 15° wing at $M = 2.0$ (figs. 5 and 6) shows that inclusion of the next mode (third bending) results in little change in the calculated flutter characteristics.

For Mach numbers above 1.65, the present results from the modified strip analysis may be compared with flutter calculations based on piston theory and on quasi-steady second-order theory for the same two wings (ref. 8). In reference 8, best overall comparisons with experiment were obtained from the quasi-steady second-order-theory calculations which included the effects of finite wing thickness. For the 15° wing, the latter calculated flutter speeds are essentially the same (within 3 percent) as those obtained herein with Busemann second-order theory. For the 30° wing, however, the best results from reference 8 compare more closely (within 9 percent) with the present calculations which employed shock-expansion theory.

Subsonic Speed Range

The subsonic flutter speeds and frequencies calculated for the 15° and 30° wings employing lifting-line aerodynamics are presented in figures 5 to 8, and for the 15° wing using lifting-surface theory in figures 5 and 6. For all cases the agreement of the calculated flutter speeds with experiment is good although the calculated frequencies are somewhat low. The flutter speeds computed for the 15° wing employing values of $c_{l_{\alpha,n}}$ and $a_{c,n}$ calculated by lifting-surface theory are somewhat lower than those obtained from values of $c_{l_{\alpha,n}}$ and $a_{c,n}$ computed by lifting-line theory. This result was expected since the local aerodynamic centers computed by lifting-surface theory are forward of those computed by lifting-line theory, and values of $c_{l_{\alpha,n}}$ computed by lifting-surface theory are larger than those computed by lifting-line theory. (See figs. 2(a), (b), and (c).)

The good agreement between the measured subsonic and supersonic flutter speeds and those calculated by the modified strip analysis (figs. 5 and 7) is of added interest in view of the high degree of bending-torsion coupling that appears in the natural vibration modes for both the 15° and 30° wings (refs. 7 and 9). It appears that for these wings the accuracy of the modified-strip-analysis calculations, which employed uncoupled vibration modes, was not adversely affected by this pronounced coupling.

CONCLUSIONS

The flutter characteristics of two untapered swept wings have been investigated analytically for Mach numbers up to 3.0. The calculations were made by a modified-strip-analysis method, employing aerodynamic parameters obtained from both linear and nonlinear aerodynamic theories. Results of the analyses and comparisons with experimental flutter data for these wings indicate the following conclusions:

1. The modified-strip-analysis method employing aerodynamic parameters obtained from shock-expansion theory, which includes the effects of airfoil shape, yields flutter speeds that are in good agreement with experimental values over the supersonic Mach number range. In comparison, the use of aerodynamic parameters calculated by the simpler Busemann second-order theory gives slightly higher calculated flutter speeds. Flutter speeds from both calculations, however, are in much better agreement with experiment than those obtained by use of linearized aerodynamic theory even at the lower Mach numbers.

2. Subsonic flutter speeds calculated for these wings by the modified-strip-analysis method with aerodynamic parameters obtained from linearized theory are in good agreement with single experimental flutter points at Mach numbers near 0.5.

Langley Research Center,
National Aeronautics and Space Administration,
Langley Station, Hampton, Va., April 22, 1963.

APPENDIX

COMPARISONS OF OSCILLATORY AERODYNAMIC LOAD DISTRIBUTIONS CALCULATED BY THE MODIFIED STRIP METHOD AND BY LINEARIZED SUPERSONIC OSCILLATING WING THEORY

Reference 20 has shown that large spanwise variations in the amplitudes and phase angles of section lift and pitching moment may occur near the tip of an oscillating wing at supersonic speeds. These results have led to questions with regard to the ability of the modified strip method to represent adequately the distributions of oscillatory aerodynamic loading over the portion of a supersonic wing which is influenced by a cut-off tip. In order to examine this question, values of oscillatory section lift and pitching moment calculated by this modified strip method have been compared with corresponding values obtained from supersonic oscillatory lifting-surface theory (ref. 20). Expressions for the load distribution on a rectangular wing oscillating as a rigid body in supersonic flow were presented in reference 20 and illustrated by calculations of the amplitudes and phase angles of the section lift and pitching moment for a wing of aspect ratio 4.0 oscillating in pitch at Mach number 1.3 (figs. 5 and 6 of ref. 20). Calculations of the loading for these conditions have also been made by the modified strip method employed in the flutter calculations of the present report. Since the loading expressions of reference 20 were based on linearized-flow theory, the steady-flow aerodynamic parameters employed in the comparative modified-strip-analysis calculations were also obtained from linear theory - that of reference 11. (See fig. 34(d) of ref. 1.)

The distributions of oscillatory aerodynamic parameters calculated by the modified strip method and those from reference 20 (fig. 9 herein) show the same general trends and magnitudes for both the amplitudes and the phase angles of the section lift and pitching moment. The amplitudes of the oscillatory section lift-curve slope calculated by the two methods are essentially identical, and the corresponding phase angles differ by less than 6°. With regard to the pitching-moment curves, however, it should be observed that the present combination of Mach number (1.30) and pitch axis (41.3 percent chord) constitute a somewhat sensitive condition for the modified-strip-theory calculation. Under these conditions the local aerodynamic centers are rather close to the pitch axis over much of the span and are actually behind the pitch axis over the inboard three-fourths of the span. The moment arms and hence the pitching moments are therefore relatively small, and the errors resulting from the approximations inherent in the modified strip method become apparent in both the amplitude and phase angle of the pitching moment. Thus, the pitching-moment phase angles θ_{cm} (fig. 9(b)) indicated by the two calculations are very close together over the outboard portion of the wing, but some differences appear inboard. Over the inboard region, both calculations yield values of θ_{cm} near 180° so that the corresponding quadrature components of the pitching moment (components in phase with the angular velocity) are shown by both methods to be relatively small compared to the components in phase with the angular displacement. However, the

inboard phase angles from the modified strip method are greater than 180°, whereas those from reference 20 are less than 180°. Thus, over the inboard region, the quadrature moment components from reference 20 would have positive sign and hence would contribute to instability, whereas those from the modified strip method would have negative sign and hence would contribute to stability. In a case such as this, use of the modified strip method in a flutter analysis would probably yield flutter speeds higher than corresponding values obtained by the method of reference 20. References 1 and 11, as well as the present report, call attention to the errors in calculated flutter speeds which may occur under such circumstances. If the pitch axis in the present calculation were farther from the local aerodynamic centers, the comparison of pitching moments (fig. 9(b)) should be improved. The comparison should also be better at lower reduced frequencies. (See ref. 1.)

REFERENCES

1. Yates, E. Carson, Jr.: Calculation of Flutter Characteristics for Finite-Span Swept or Unswept Wings at Subsonic and Supersonic Speeds by a Modified Strip Analysis. NACA RM L57L10, 1958.

2. Shapiro, Ascher H.: The Dynamics and Thermodynamics of Compressible Fluid Flow. Vol. I. The Ronald Press Co., c.1953, pp. 575-576.

3. Katzen, Elliott D., and Pitts, William C.: Load Distributions on Wings and Wing-Body Combinations at High Angles of Attack and Supersonic Speeds. NACA RM A55E17, 1955.

4. Katzen, Elliott D.: Limitations of Linear Theory in Predicting the Pressure Distribution on Triangular Wings. Jour. Aero. Sci. (Readers' Forum), vol. 22, no. 7, July 1955, pp. 514-515.

5. Yates, E. Carson, Jr.: Some Effects of Variations in Density and Aerodynamic Parameters on the Calculated Flutter Characteristics of Finite-Span Swept and Unswept Wings at Subsonic and Supersonic Speeds. NASA TM X-182, 1960.

6. Yates, E. Carson, Jr.: Use of Experimental Steady-Flow Aerodynamic Parameters in the Calculation of Flutter Characteristics for Finite-Span Swept or Unswept Wings at Subsonic, Transonic, and Supersonic Speeds. NASA TM X-183, 1960.

7. Tuovila, W. J., and McCarty, John Locke: Experimental Flutter Results for Cantilever-Wing Models at Mach Numbers up to 3.0. NACA RM L55E11, 1955.

8. Bennett, Robert M., and Yates, E. Carson, Jr.: A Study of Several Factors Affecting the Flutter Characteristics Calculated for Two Swept Wings by Piston Theory and by Quasi-Steady Second-Order Theory and Comparison With Experiments. NASA TN D-1794, 1963.

9. Hanson, Perry W., and Tuovila, W. J.: Experimentally Determined Natural Vibration Modes of Some Cantilever-Wing Flutter Models by Using an Acceleration Method. NACA TN 4010, 1957.

10. Yates, E. Carson, Jr.: Subsonic and Supersonic Flutter Analysis of a Highly Tapered Swept-Wing Planform, Including Effects of Density Variation and Finite Wing Thickness, and Comparison With Experiments. NASA TM X-764, 1963.

11. Lagerstrom, P. A., Wall, D., and Graham, M. E.: Formulas in Three-Dimensional Wing Theory. Rep. No. SM-11901, Douglas Aircraft Co., Inc., July 8, 1946.

12. Yates, E. Carson, Jr.: Theoretical Analysis of Linked Leading-Edge and Trailing-Edge Flap-Type Controls at Supersonic Speeds. NACA TN 3617, 1956.

13. Goin, Kennith L.: Equations and Charts for the Rapid Estimation of Hinge-Moment and Effectiveness Parameters for Trailing-Edge Controls Having Leading and Trailing Edges Swept Ahead of the Mach Lines. NACA Rep. 1041, 1951. (Supersedes NACA TN 2221.)

14. Ames Research Staff: Equations, Tables, and Charts for Compressible Flow. NACA Rep. 1135, 1953. (Supersedes NACA TN 1428.)

15. Pitts, William C.: Force, Moment, and Pressure-Distribution Characteristics of Rectangular Wings at High Angles of Attack and Supersonic Speeds. NACA RM A55K09, 1956.

16. Baradell, Donald L., and Bertram, Mitchel H.: The Blunt Plate in Hypersonic Flow. NASA TN D-408, 1960.

17. DeYoung, John, and Harper, Charles W.: Theoretical Symmetric Span Loading at Subsonic Speeds for Wings Having Arbitrary Plan Form. NACA Rep. 921, 1948.

18. Falkner, V. M.: The Calculation of Aerodynamic Loading on Surfaces of Any Shape. R & M No. 1910, British A.R.C., Aug. 1943.

19. Lighthill, M. J.: Higher Approximations. General Theory of High Speed Aerodynamics. Vol. VI of High Speed Aerodynamics and Jet Propulsion, sec. E, W. R. Sears, ed., Princeton Univ. Press, 1954, pp. 345-489.

20. Nelson, Herbert C., Rainey, Ruby A., and Watkins, Charles E.: Lift and Moment Coefficients Expanded to the Seventh Power of Frequency for Oscillating Rectangular Wings in Supersonic Flow and Applied to a Specific Flutter Problem. NACA TN 3076, 1954.

TABLE I.- MODAL FREQUENCIES AND FLUTTER TEST CONDITIONS

(a) Wing with 15° sweepback

Model	Material	Coupled mode frequencies			Uncoupled mode frequencies				Test conditions			
		ω_1, radians/sec	ω_2, radians/sec	ω_3, radians/sec	$\omega_{h,1}$ radians/sec	$\omega_{h,2}$ radians/sec	$\omega_{h,3}$ radians/sec	ω_α, radians/sec	M	ρ, slug/cu ft	$\bar{\mu}$	k
A	Magnesium	232	1,370	1,696	245	1,537	-----	1,456	3.00	0.00093	79	0.0390
B	Magnesium	220	1,288	1,470	232	1,454	4,071	1,377	2.00	.00053	139	.0432
C	Aluminum	226	1,319	1,596	251	1,575	-----	1,488	1.30	.00049	234	.0432
D	Aluminum	226	1,319	1,520	251	1,575	-----	1,488	.45	.0023	50	.1314

(b) Wing with 30° sweepback

Model	Material	Coupled mode frequencies			Uncoupled mode frequencies			Test conditions			
		ω_1, radians/sec	ω_2, radians/sec	ω_3, radians/sec	$\omega_{h,1}$ radians/sec	$\omega_{h,2}$ radians/sec	ω_α, radians/sec	M	ρ, slug/cu ft	$\bar{\mu}$	k
A	Magnesium	264	1,351	1,866	260	1,629	1,496	3.00	0.00067	100	0.0470
B	Magnesium	239	1,319	1,640	235	1,473	1,353	2.00	.00043	156	.0511
C	Aluminum	245	1,319	1,721	267	1,673	1,533	1.30	.00044	234	.0444
D	Aluminum	220	1,319	1,696	240	1,501	1,376	.47	.0023	45	.1403

TABLE II.- SUMMARY OF FLUTTER CALCULATIONS

Vibration modes (uncoupled)	Mach number	Aerodynamic parameters		15° swept wing			30° swept wing		
		Theory	Finite thickness	Model	Results shown in figure -		Model	Results shown in figure -	
					$\frac{V}{b_s\omega_\alpha\sqrt{\bar{\mu}}}$	ω/ω_α		$\frac{V}{b_s\omega_\alpha\sqrt{\bar{\mu}}}$	ω/ω_α
Supersonic									
3	1.15 to 3.00	Linear lifting surface (ref. 11)	No	A, B, C	5	6	A, B, C	7	8
	1.33 to 3.00	Shock expansion (ref. 14)	Yes	A, B, C	5	6	A, B, C	7	8
	2.00 to 3.00	Busemann second order (ref. 19)	Yes	A, B, C	5	6	A, B	7	8
4	2.00	Shock expansion (ref. 14)	Yes	B	5	6	-------	---	---
Subsonic									
3	0 to 0.75	Lifting line (ref. 17)	No	D	5	6	D	7	8
		Lifting surface (ref. 18)	No	D	5	6	-------	---	---

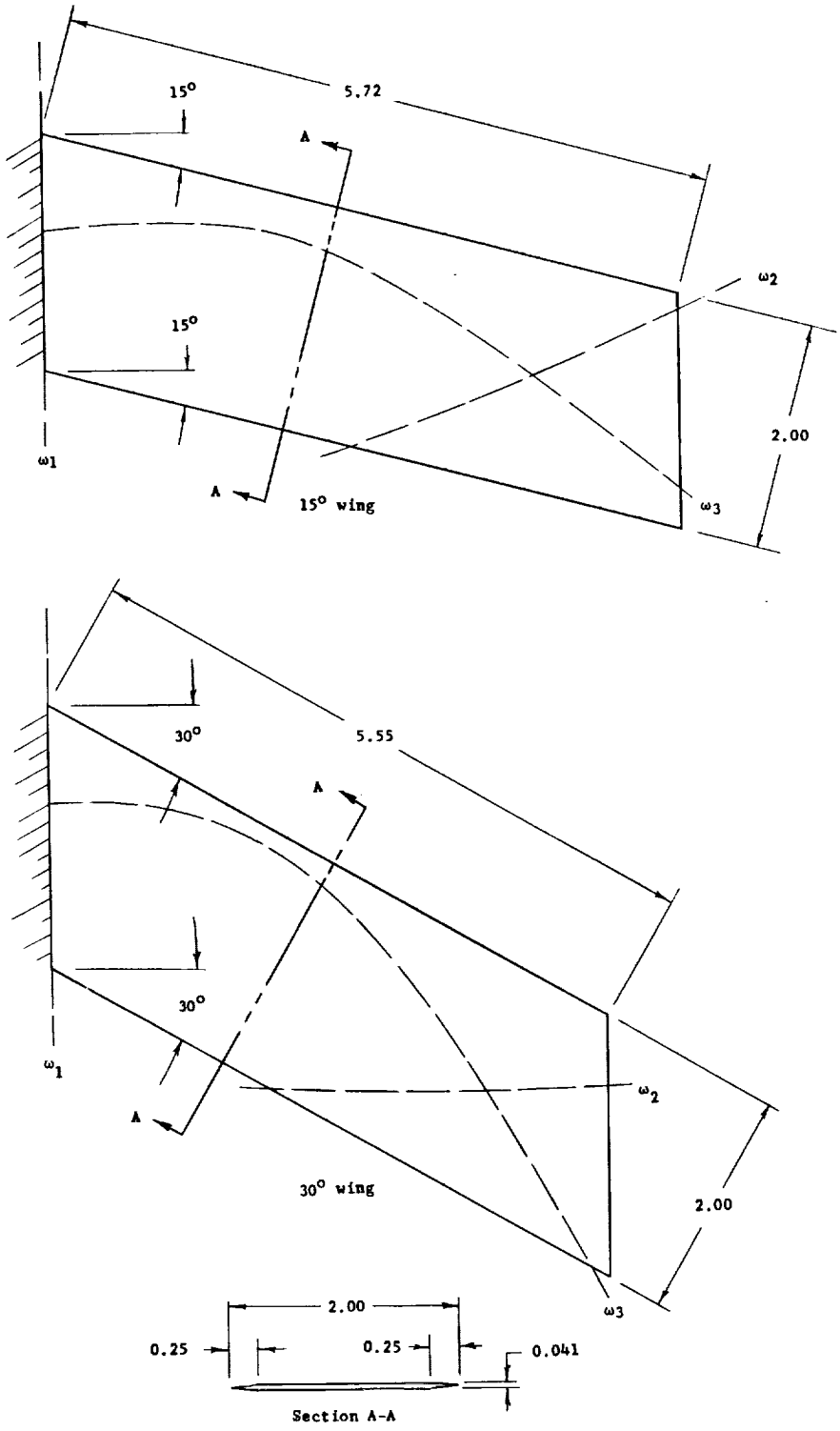

Figure 1.- Sketch of wing planforms showing measured node lines. All dimensions are in inches unless otherwise specified.

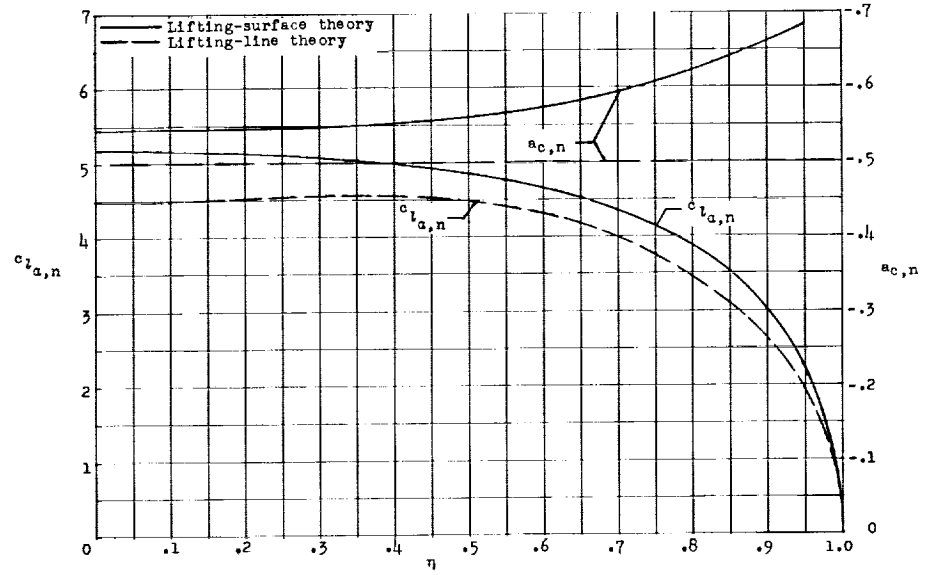

(a) M = 0.

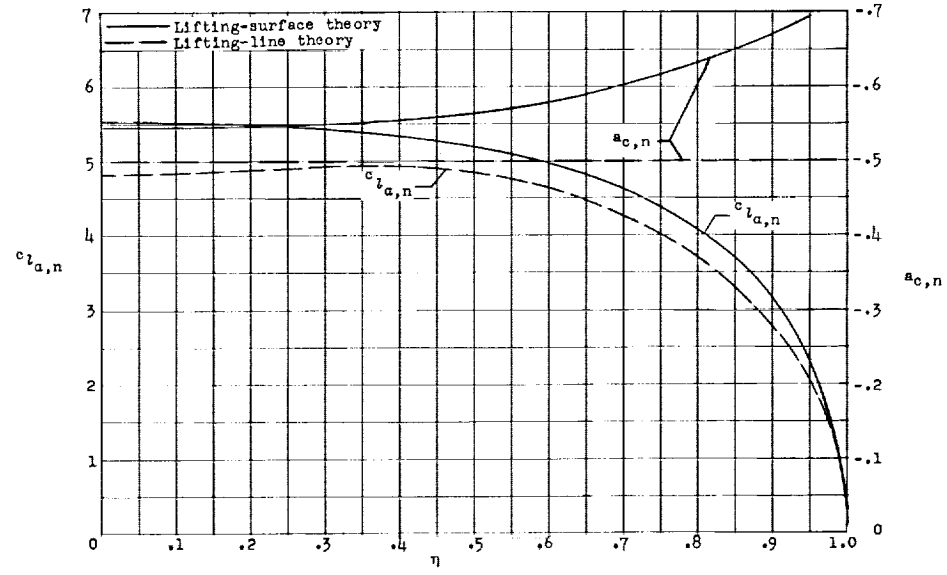

(b) M = 0.45.

Figure 2.- Distributions of static aerodynamic parameters for the 15° wing.

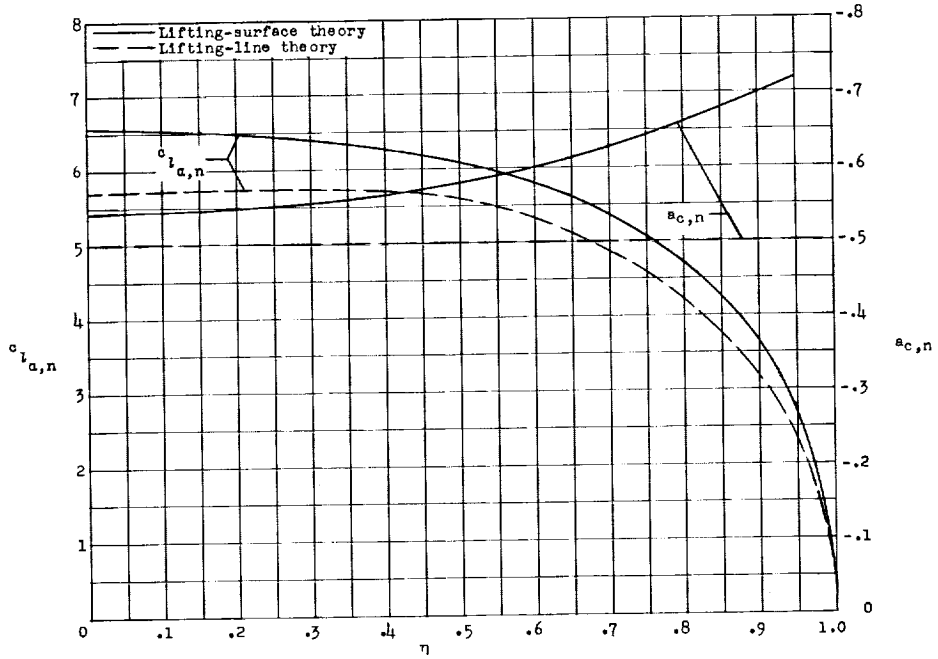

(c) M = 0.75.

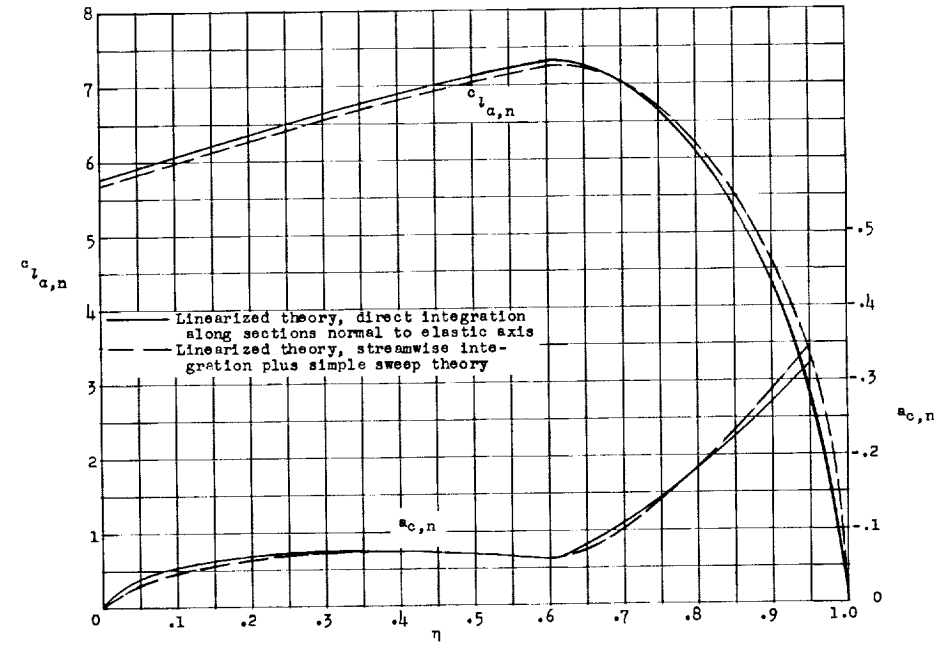

(d) M = 1.15470.

Figure 2.- Continued.

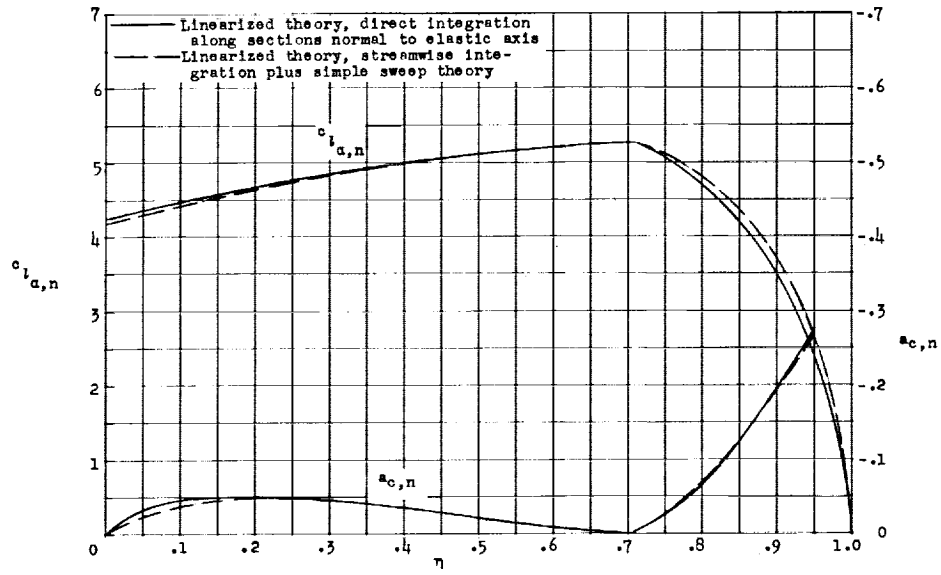

(e) M = 1.30.

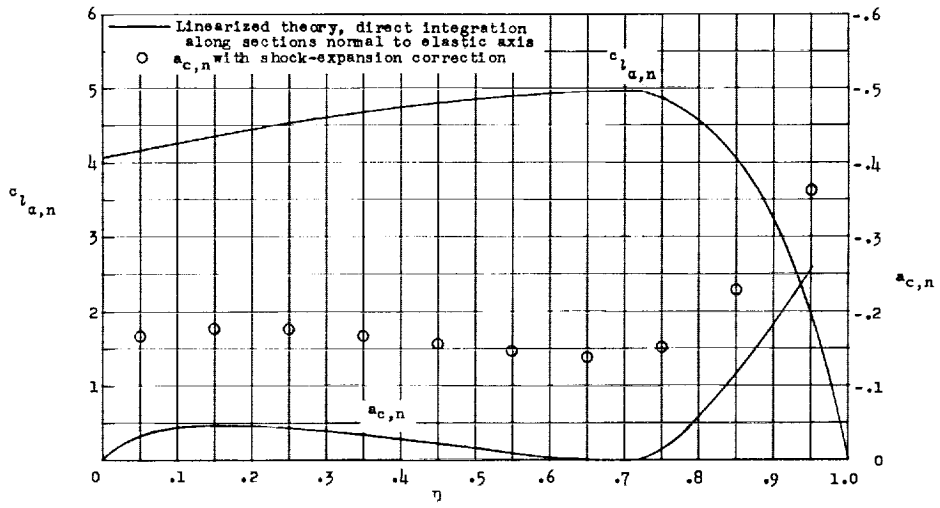

(f) M = 1.33.

Figure 2.- Continued.

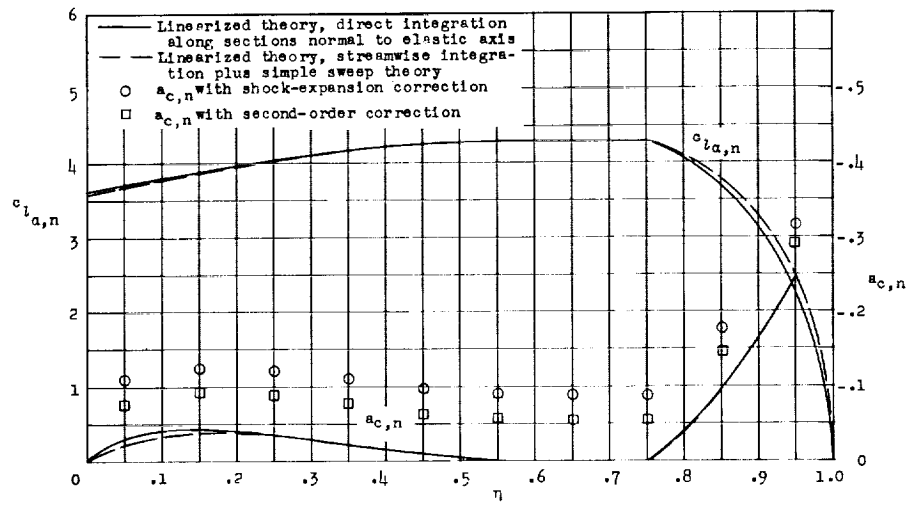

(g) $M = \sqrt{2}$.

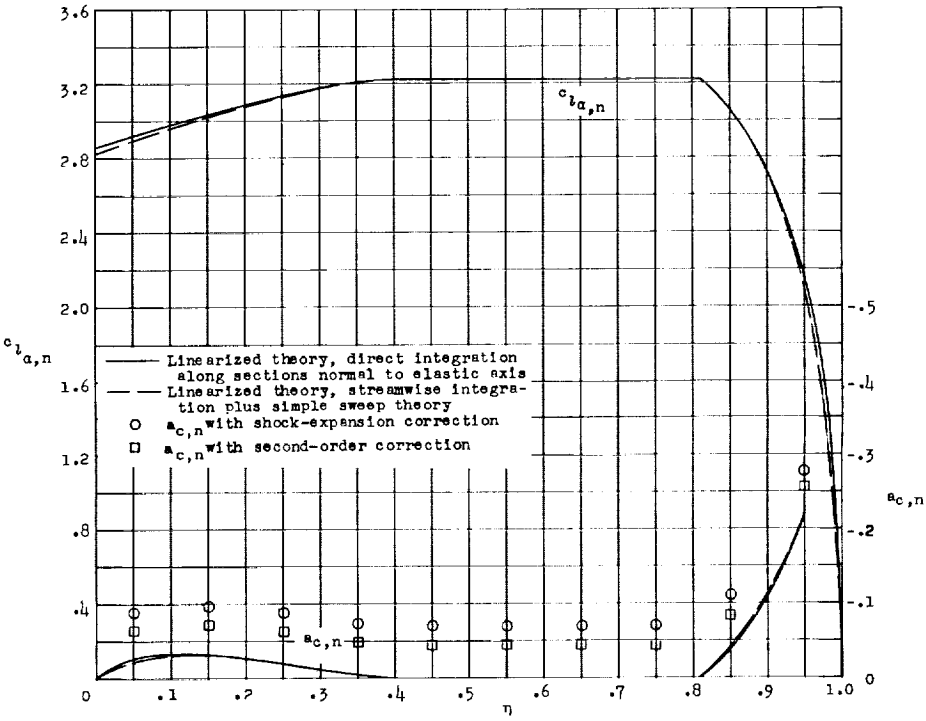

(h) $M = 1.65$.

Figure 2.- Continued.

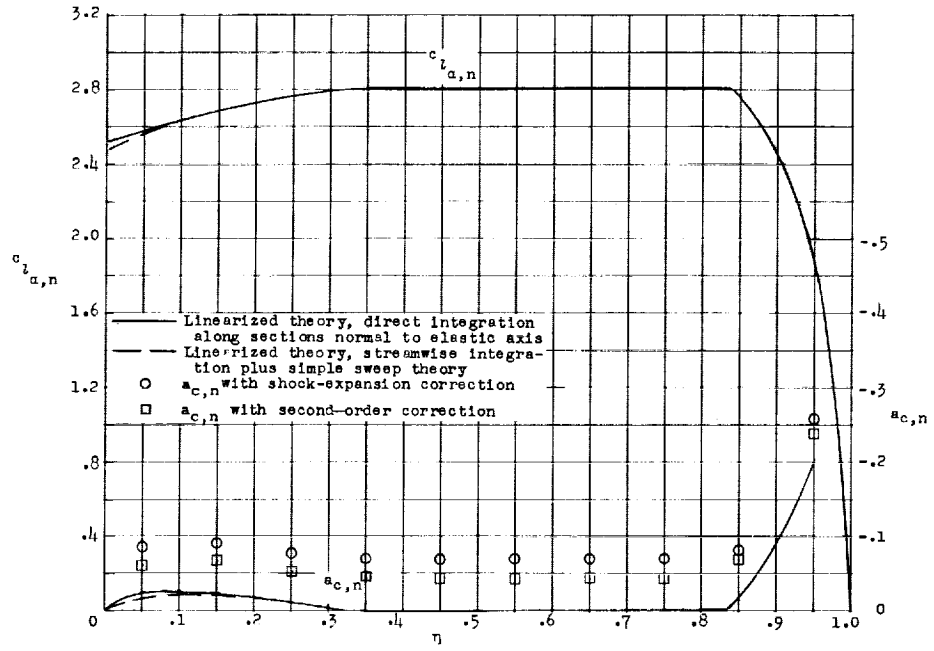

(i) M = 1.80.

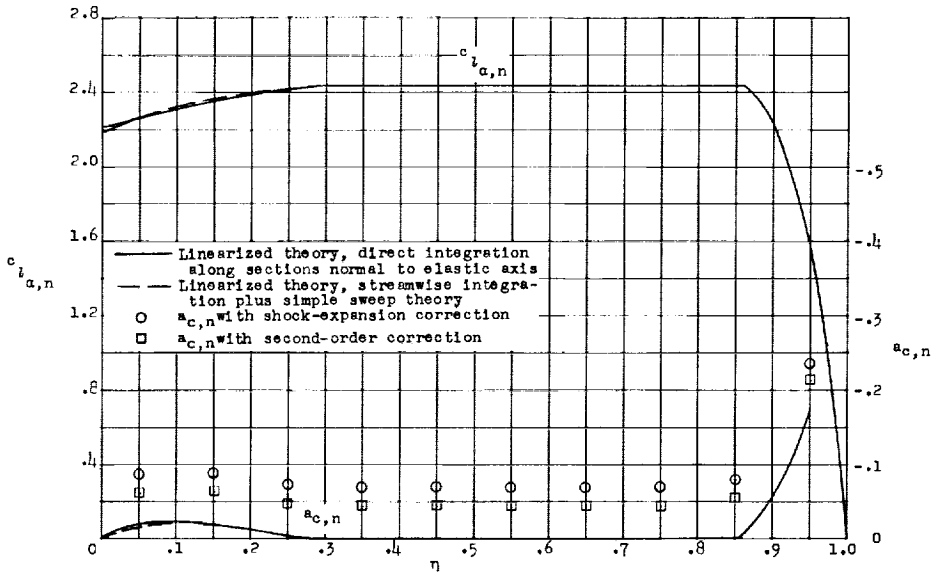

(j) M = 2.00.

Figure 2.- Continued.

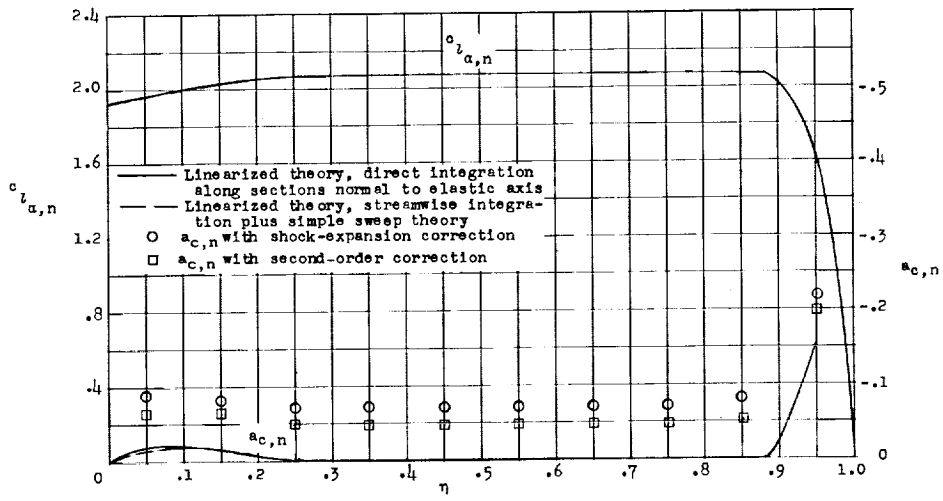

(k) M = 2.25.

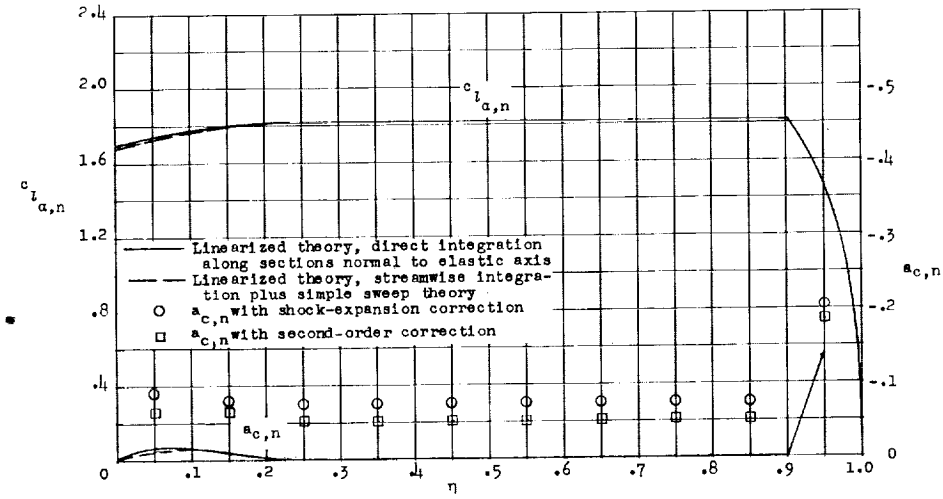

(l) M = 2.50.

Figure 2.- Continued.

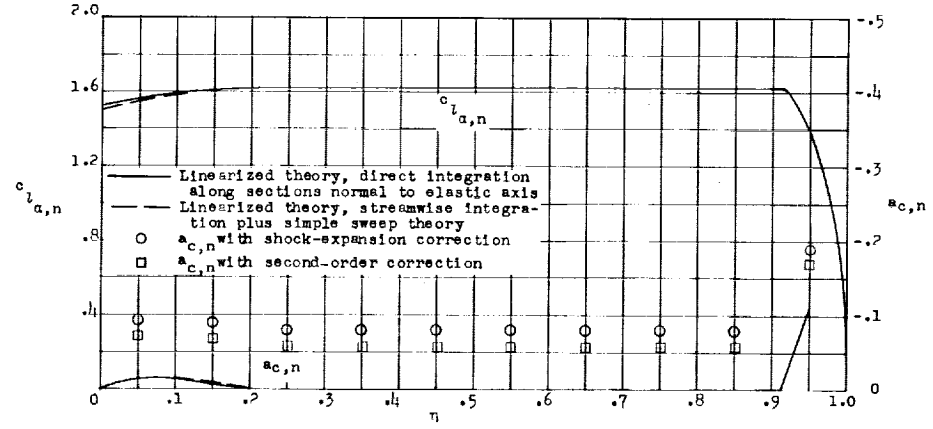

(m) M = 2.75.

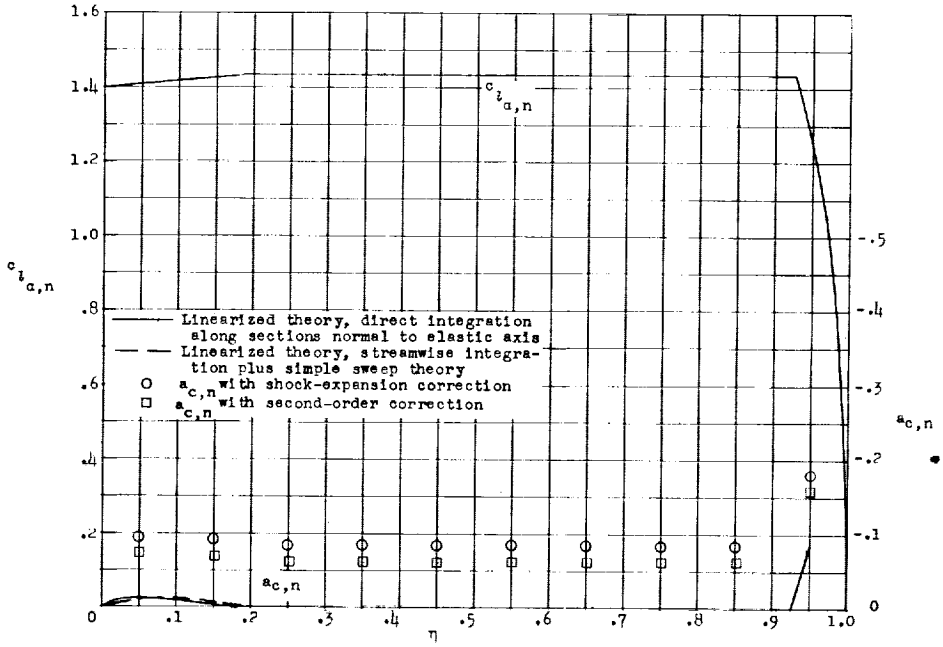

(n) M = 3.00.

Figure 2.- Concluded.

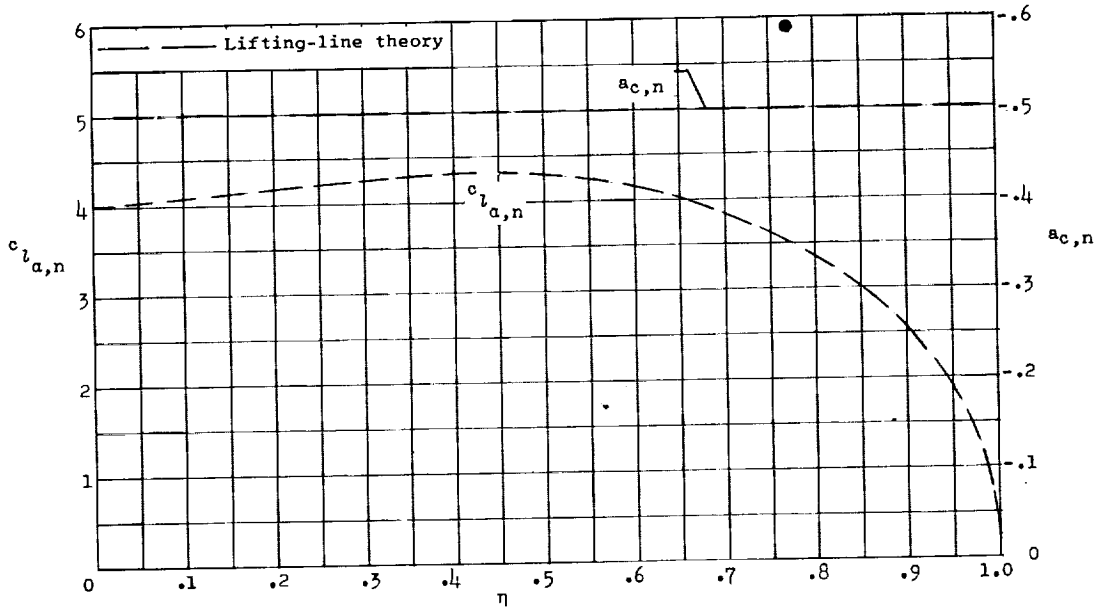

(a) M = 0.

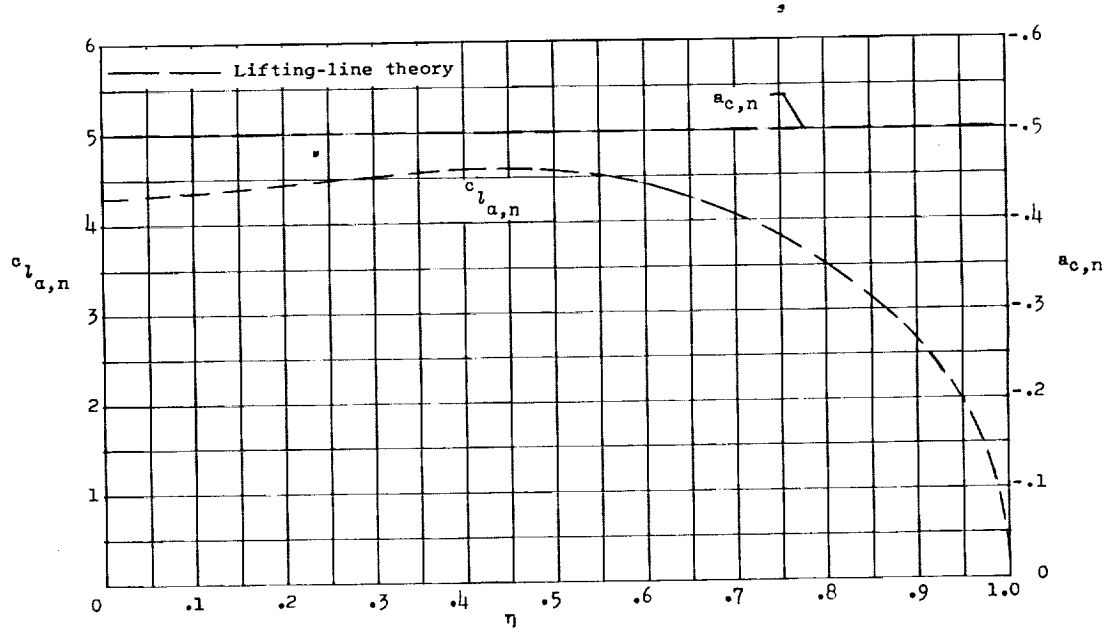

(b) M = 0.47.

Figure 3.- Distributions of static aerodynamic parameters for the 30° wing.

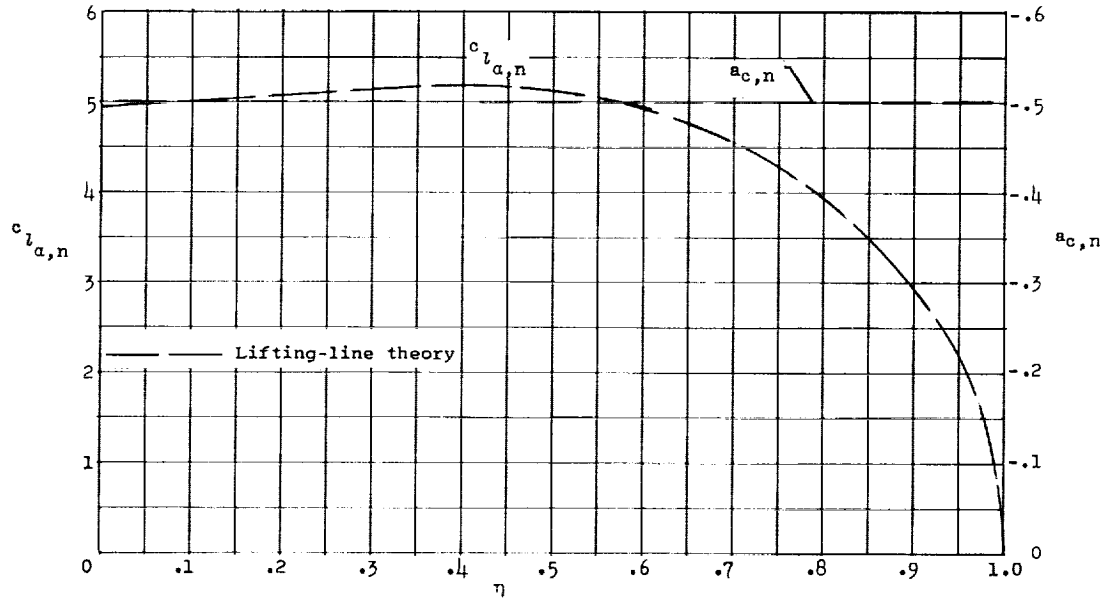

(c) M = 0.75.

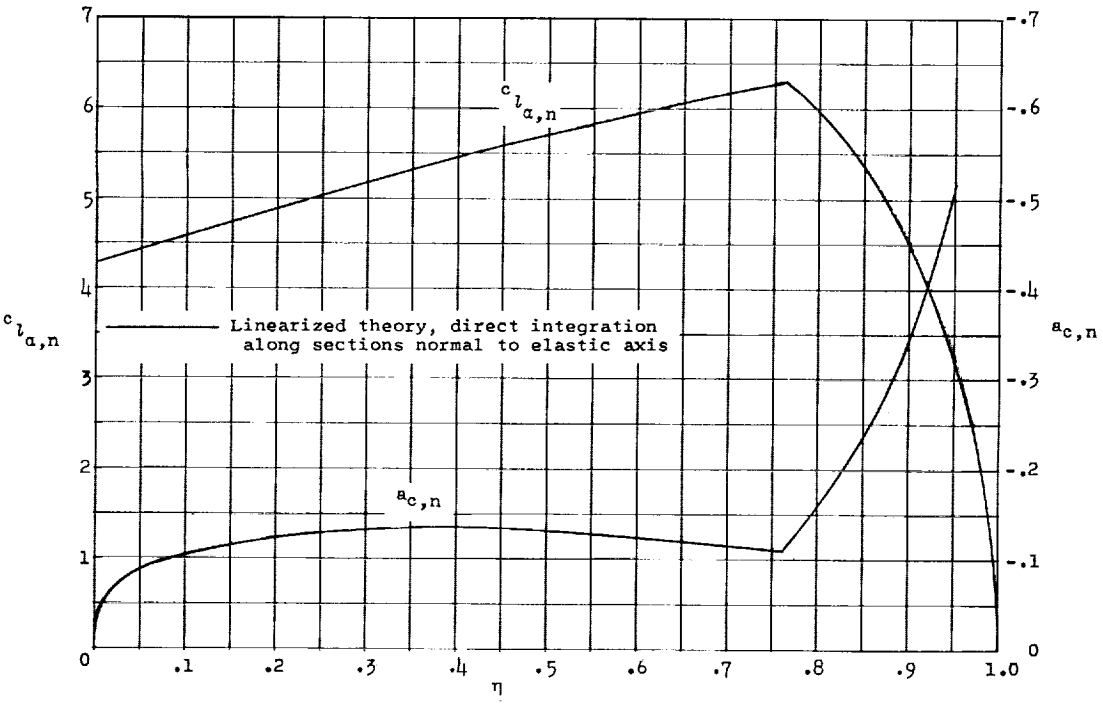

(d) M = 1.30.

Figure 3.- Continued.

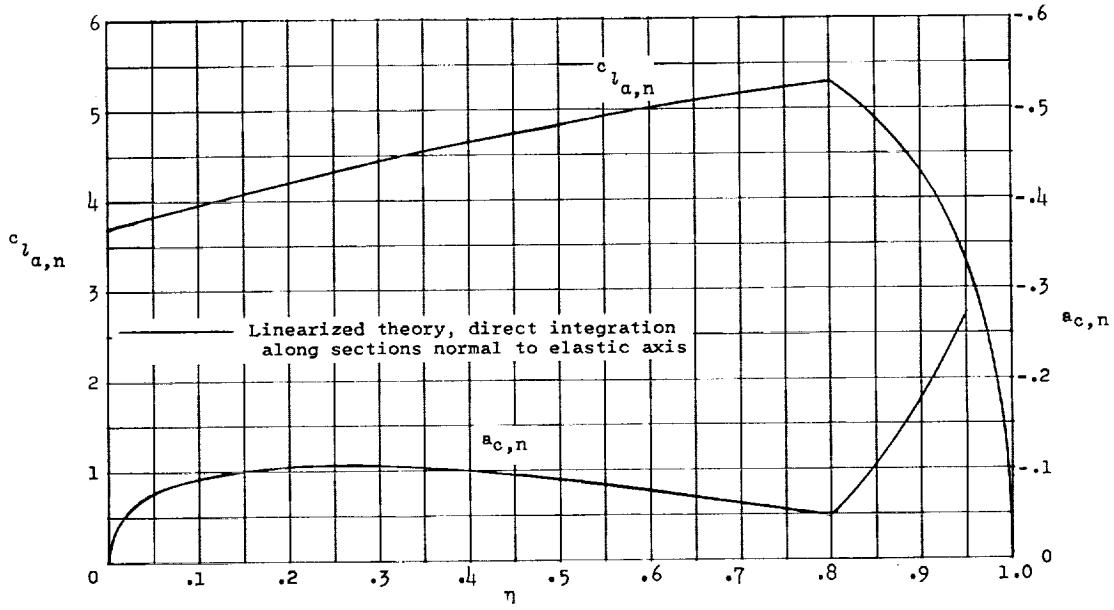

(e) $M = \sqrt{2}$.

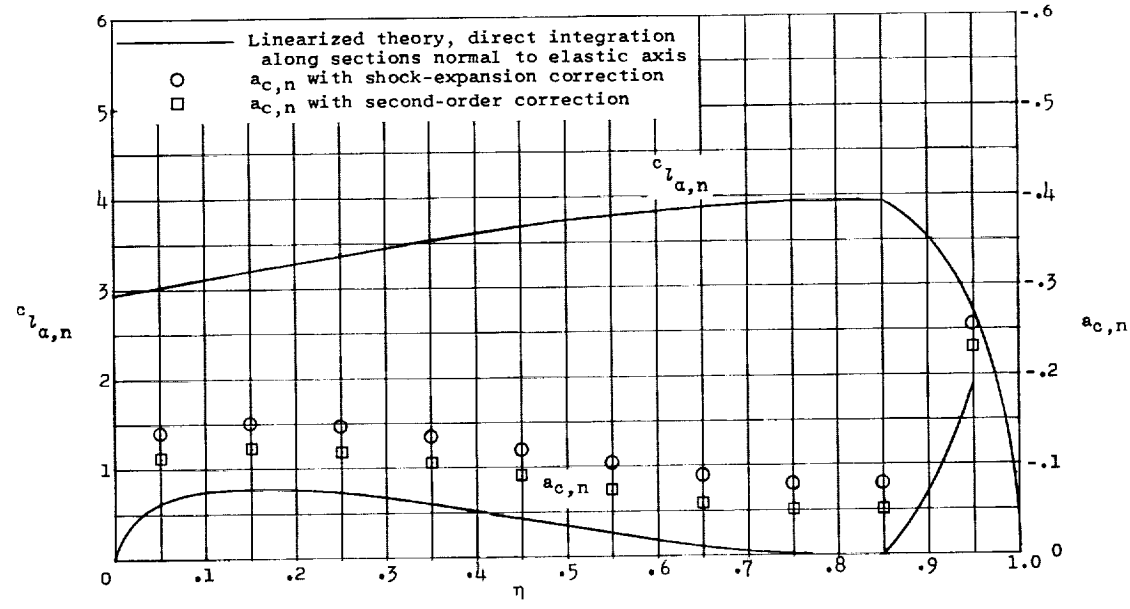

(f) $M = 1.65$.

Figure 3.- Continued.

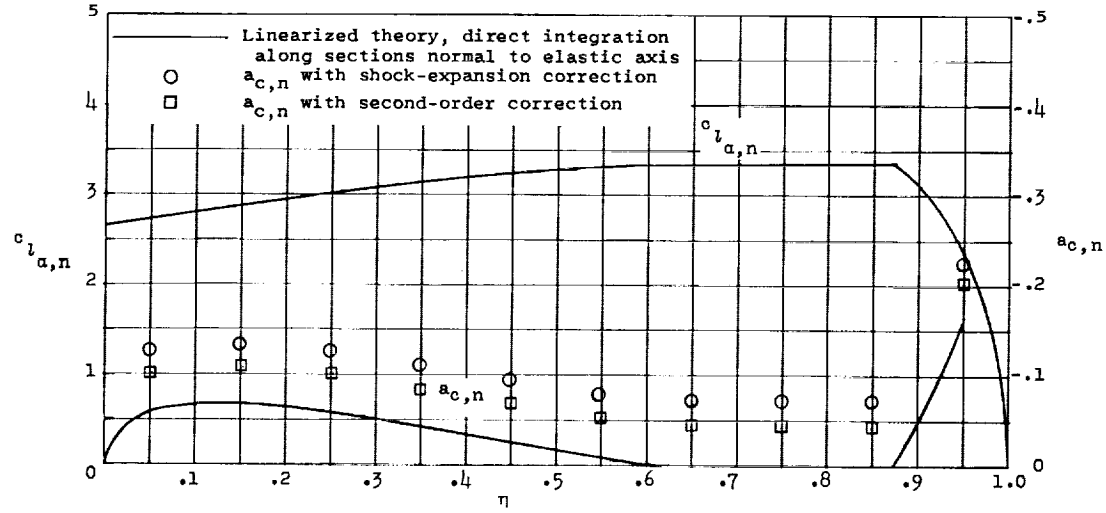

(g) M = 1.80.

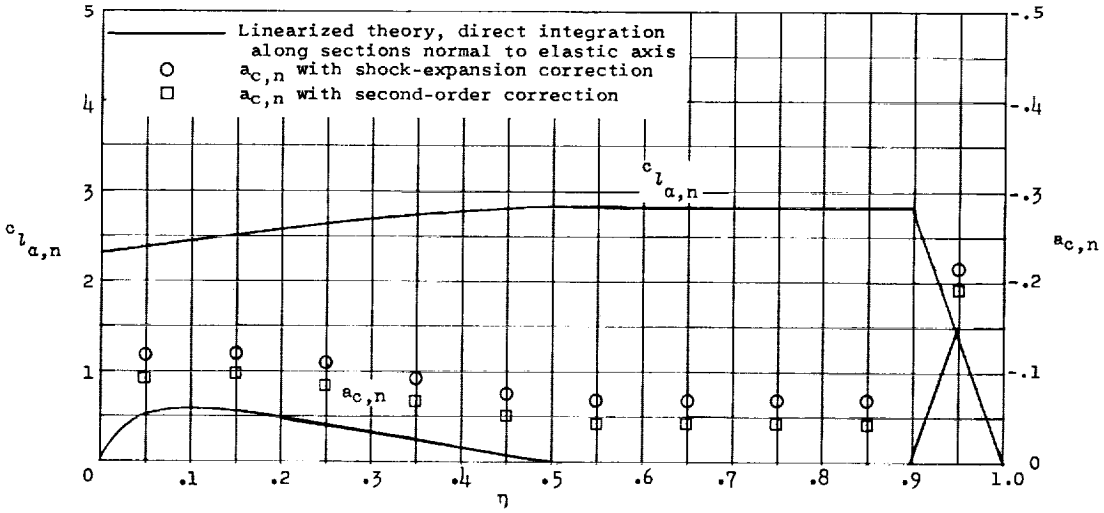

(h) M = 2.00.

Figure 3.- Continued.

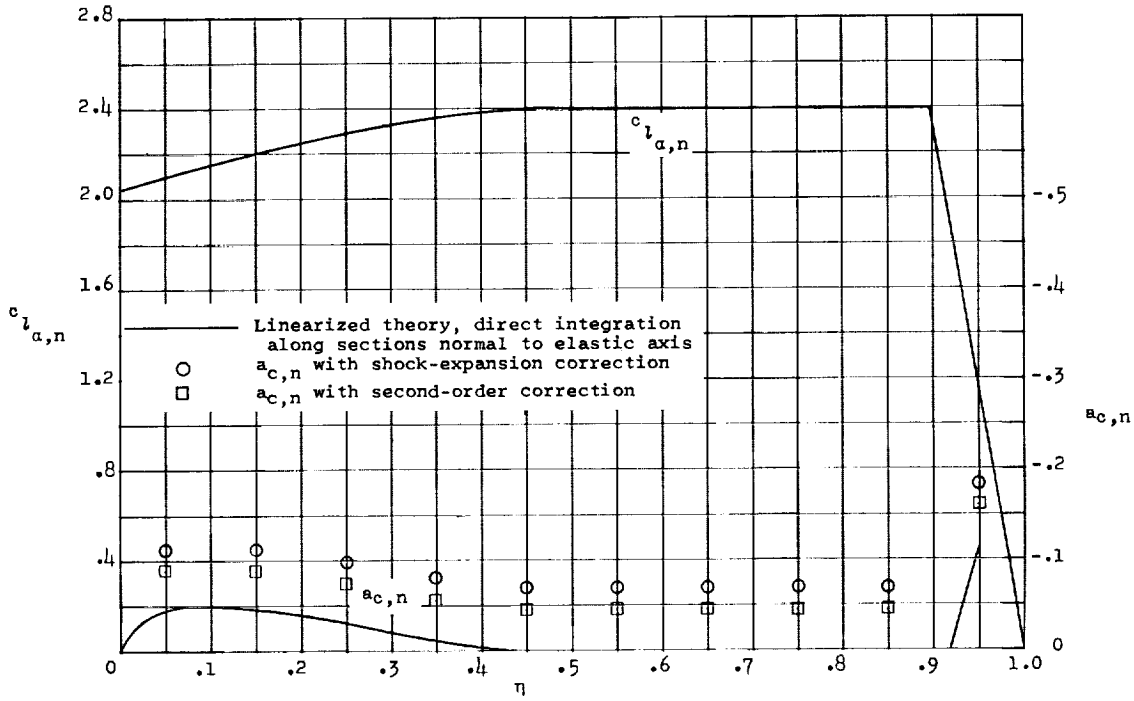

(i) M = 2.25.

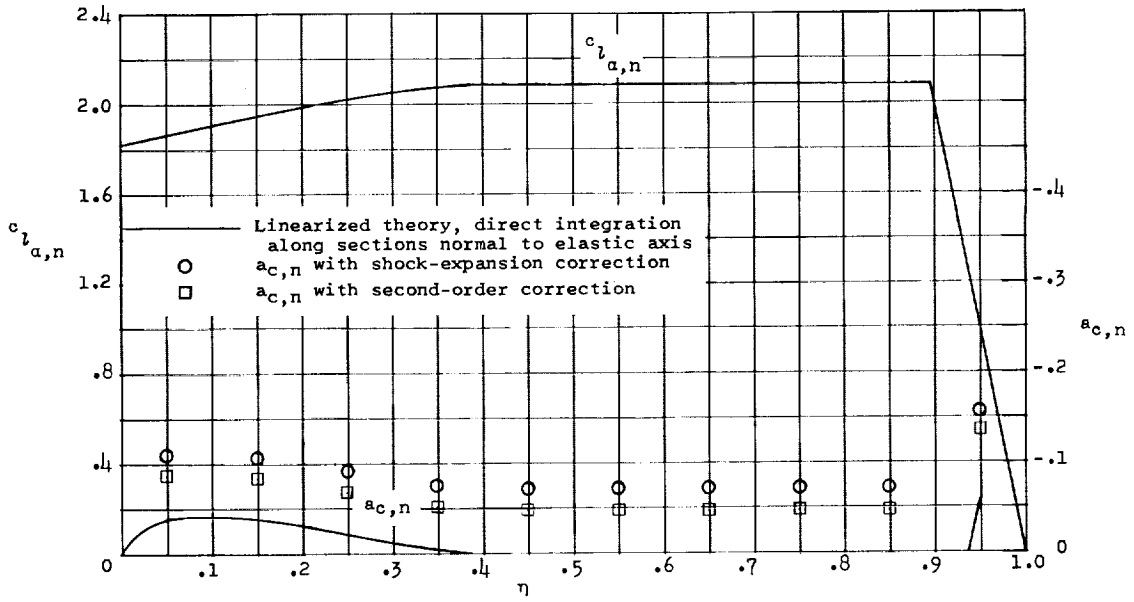

(j) M = 2.50.

Figure 3.- Continued.

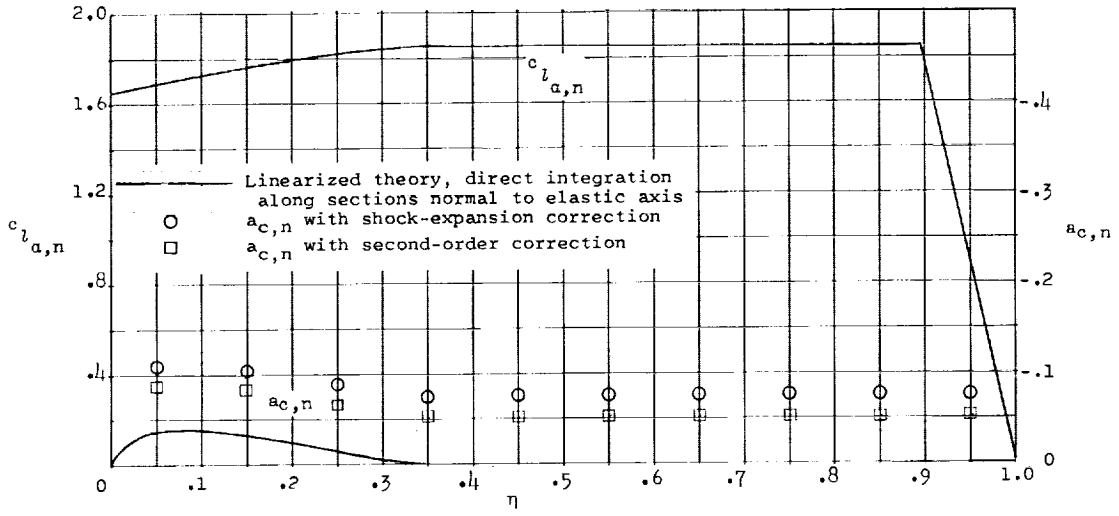

(k) M = 2.75.

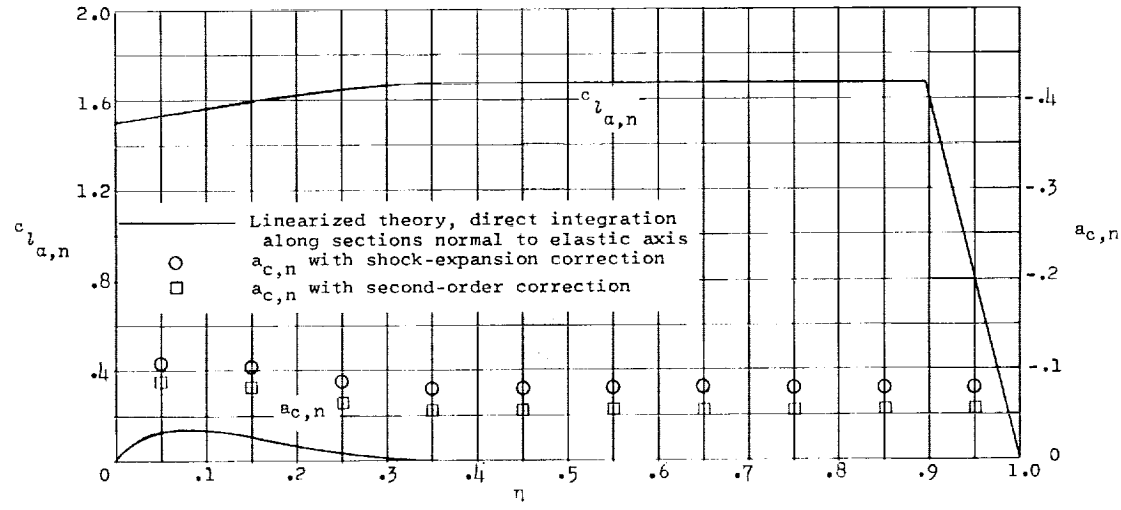

(l) M = 3.00.

Figure 3.- Concluded.

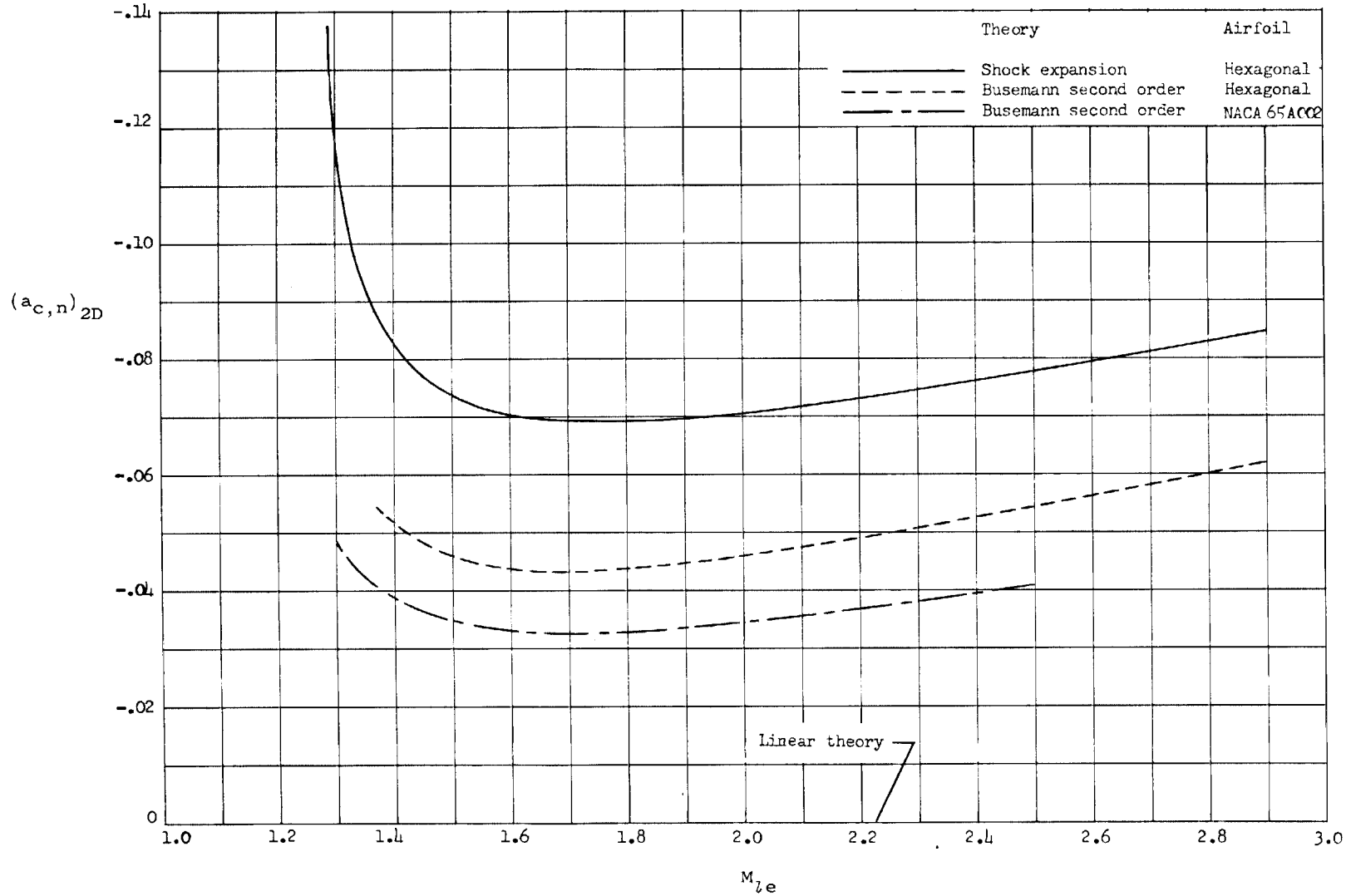

Figure 4.- Aerodynamic center for two-dimensional flow.

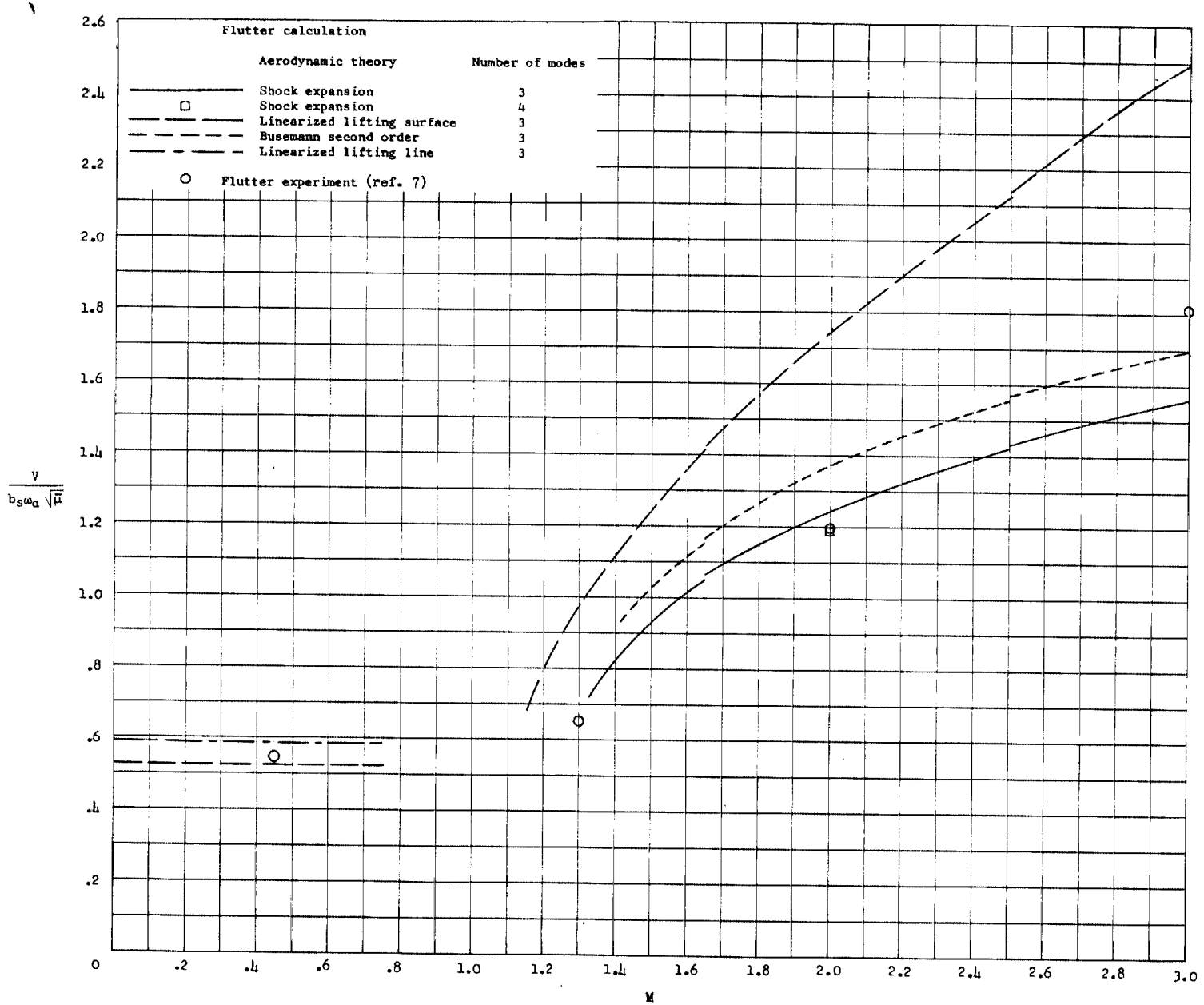

Figure 5.- Variation of flutter-speed coefficient with Mach number for the 15° wing.

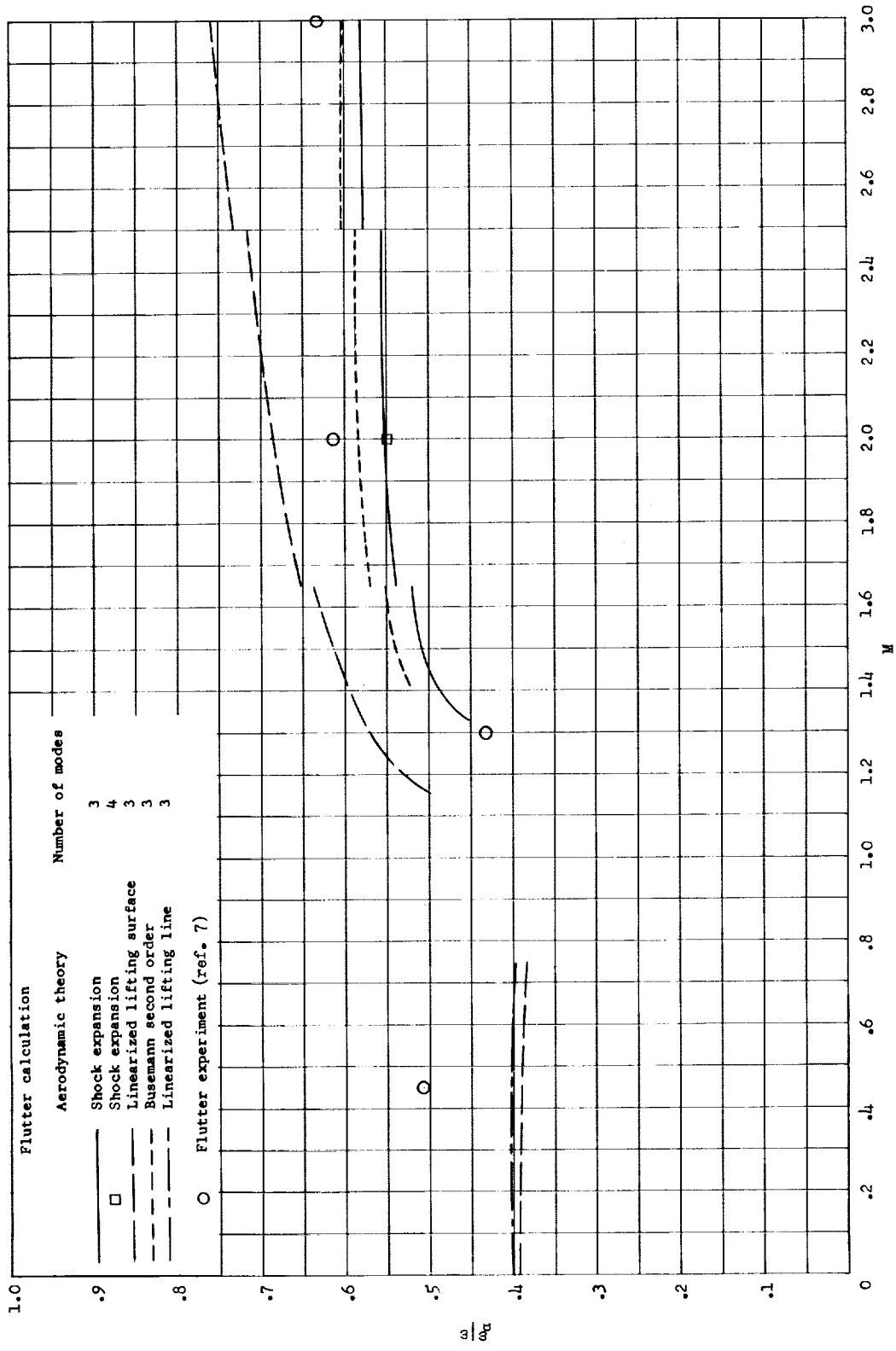

Figure 6.- Variation of flutter frequency with Mach number for the 15° wing.

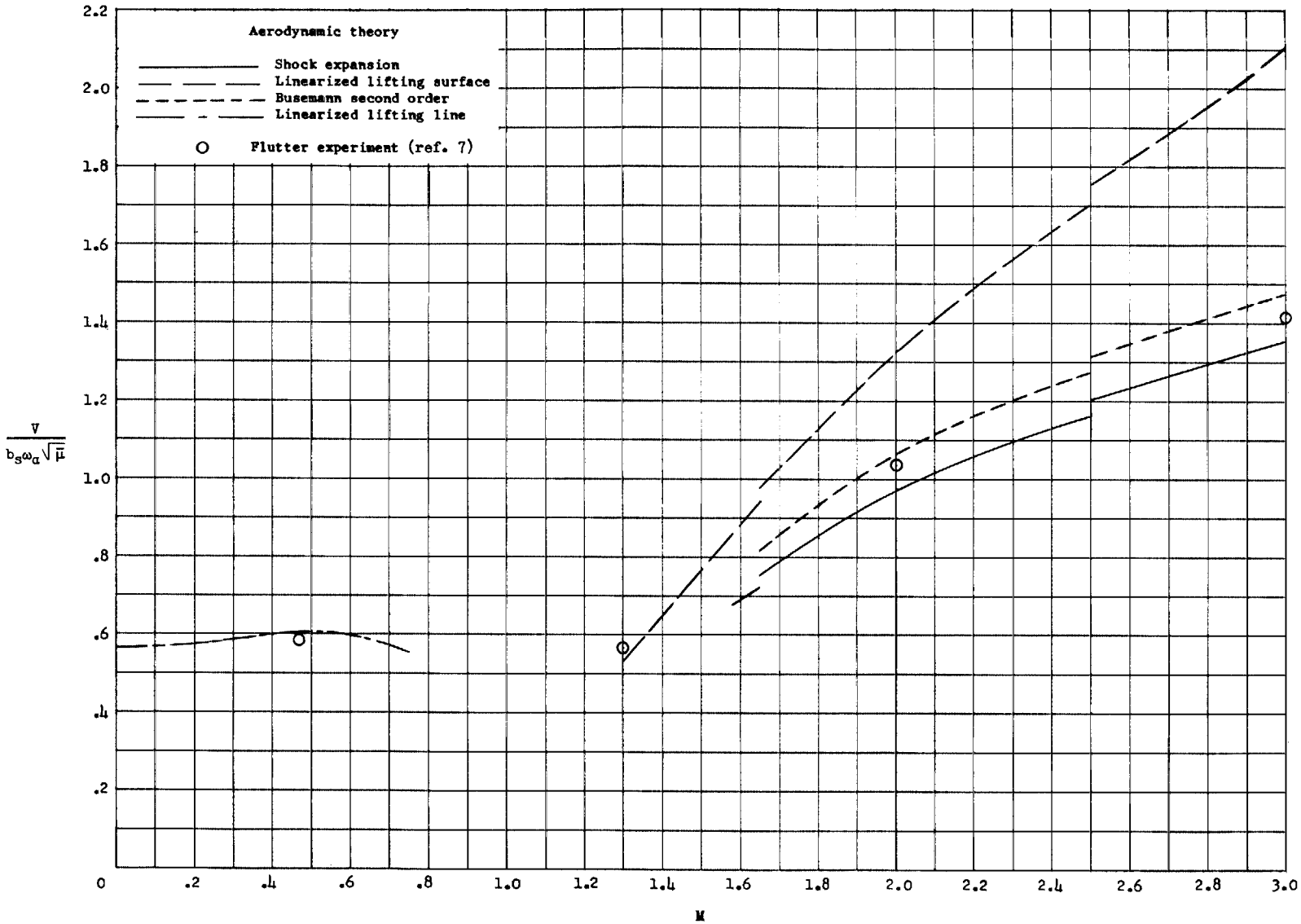

Figure 7.- Variation of flutter-speed coefficient with Mach number for the 30° wing. All calculations were made with three vibration modes.

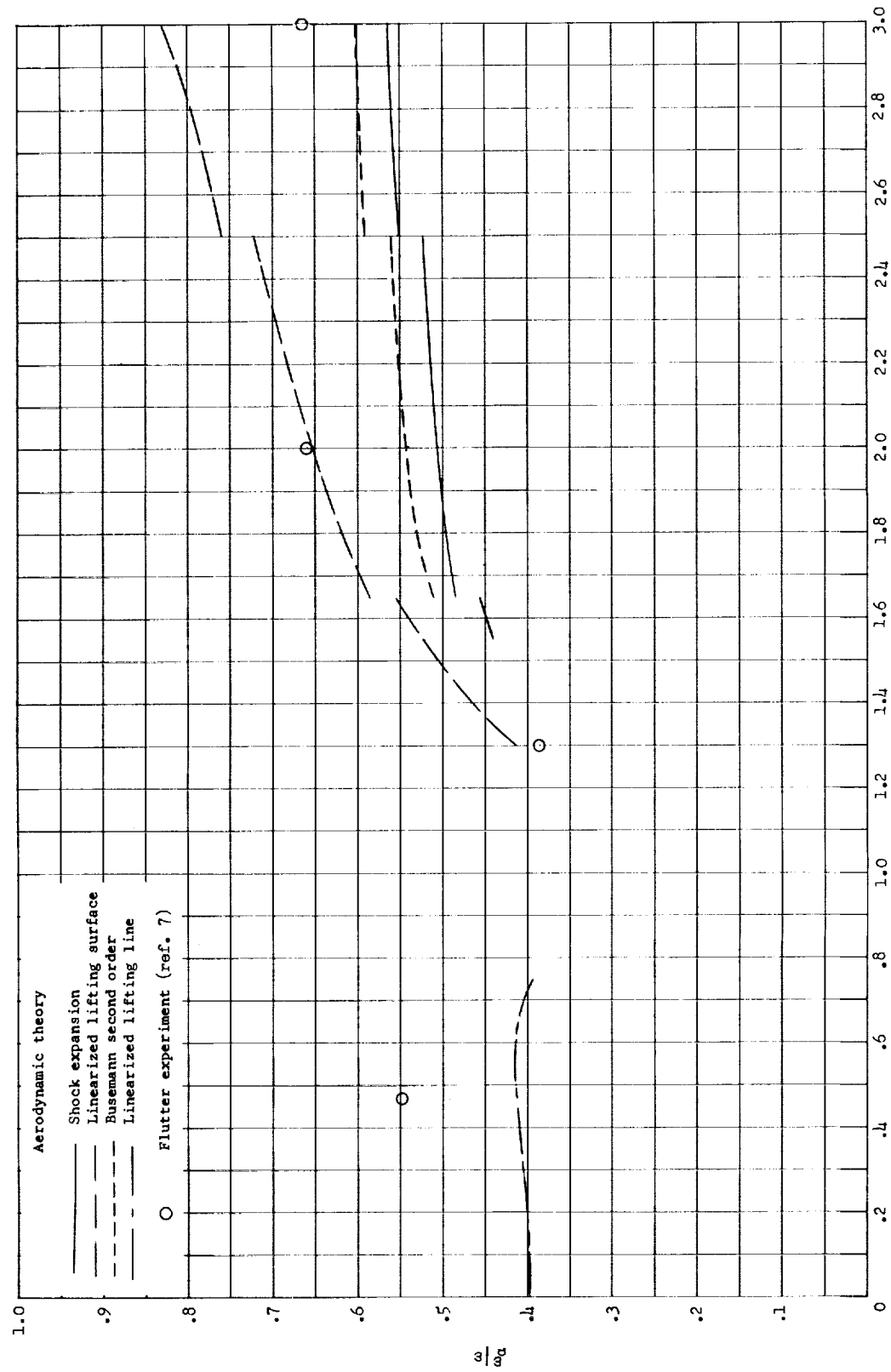

Figure 8.- Variation of flutter frequency with Mach number for the 30° wing. All calculations were made with three vibration modes.

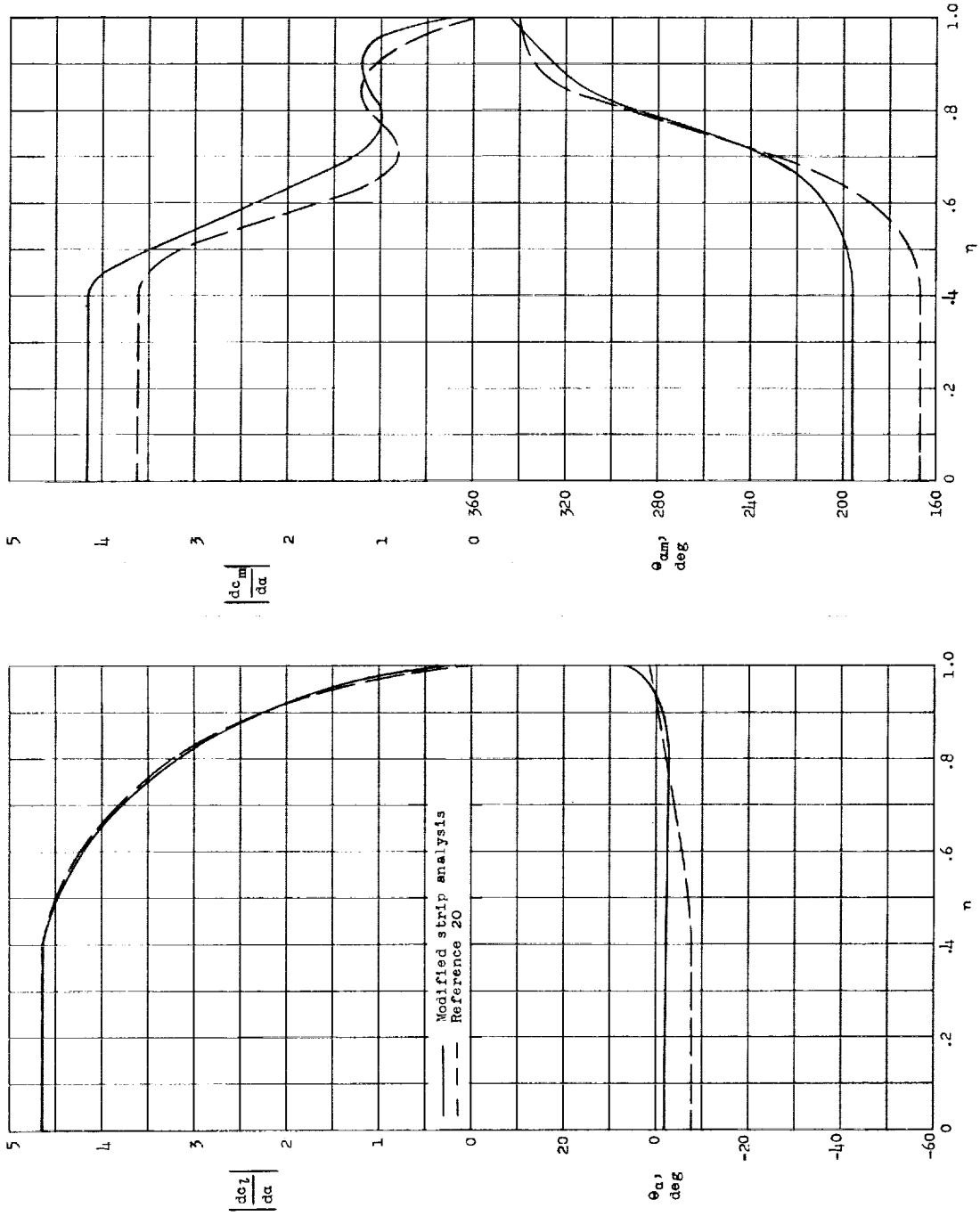

(a) Section lift coefficient.

(b) Section pitching-moment coefficient.

Figure 9.- Oscillatory aerodynamic load distributions calculated by modified strip method and by linearized supersonic oscillating lifting-surface theory for rectangular wing of aspect ratio 4.0 oscillating as a rigid body in pitch. Pitch axis is located 41.3 percent chord from leading edge; M = 1.3; k = 0.111.